ADDIS ABABA UNIVERSITY

ADDIS ABABA INSTITUTE OF TECHNOLOGY

SCHOOL OF CIVIL AND ENVIRONMENTAL ENGINEERING



Effects of Spacing and Configuration of Web Reinforcement on Shear Behavior of Reinforced Concrete Beams

A Thesis in Structural Engineering

By Mekdes Tadesse

12/12/2015

Addis Ababa

Submitted in Partial Fulfillment of the Requirements for the Degree of Master of Science

ADDIS ABABA UNIVERSITY

ADDIS ABABA INSTITUTE OF TECHNOLOGY

SCHOOL OF CIVIL AND ENVIRONMENTAL ENGINEERING

"Effects of Spacing and Configuration of Web Reinforcement on shear Behavior of Reinforced Concrete Beams"

By

Mekdes Tadesse

Approved by the Board of Examiners:

Dr. Esayas G/Youhannes		
Advisor	**Signature**	**Date**
Dr. Ing. Adil Zekaria		
Internal Examiner	**Signature**	**Date**
Dr. Ing. Girma Zerayohannes		
External Examiner	**Signature**	**Date**

ACKNOWLEDGMENTS

First I would like to thank God for his blessings and for helping me achieve success in every endeavor of my life. I would also like to thank my family for their guidance and encouragement throughout my personal life and professional career.

My sincere gratitude goes to my advisor who is also my inspiration, Dr. Esayas G/Youhannes, for his guidance, continuous support and remarkable patience throughout my research. His trust and confidence in me has helped me succeed in this challenge. My sincere gratitude goes to Chair of Concrete materials and structures, Dr. Girma Zerayouhannes for his valuable inputs and help throughout my course of graduate studies. My appreciation is extended to Dr. Adil Zekaria for giving me an interest in reinforced concrete since my undergraduate study. His support and encouragement in my structural engineering study and most of all his fatherly approach and guidance is priceless.

I would like to express my heartfelt gratitude to Dr Abrham G. for his guidance during the experiment.

I would like to take this opportunity to express my heartfelt appreciation to my esteemed colleagues Abinet, Alelegn B, Derese B, Eyuel M , Fresenay Z, Habtamu A, Selamawit D, Simon M, and Samson W for giving me all the support I needed throughout the Experimental program. Without their support and encouragement, the experimental program wouldn't have been a reality. I am grateful to Fikru B. and Wubet A. in the construction materials testing laboratory for assisting me in many different ways.

I would like to thank my friends Hana M. and Eyuel M. for all the support they offered and for helping me get through the difficult times.

My sincere appreciation goes to my students Robel B. and Abel S. for their support during the experiment.

Last but not least I would like to thank Anchor Foundation specialist p.l.c. and my friend Semon Tegegn for supplying me with High strength reinforcement bars.

TABLE OF CONTENTS

LIST OF TABLES ..... **IV**

LIST OF FIGURES ..... **V**

ABSTRACT **1**

CHAPTER 1 INTRODUCTION **2**

1.1 General Background 2
1.2 Significance 4
1.3 Objectives 4
1.4 Scope 4
1.5 Methodology 5

CHAPTER 2 LITERATURE REVIEW **6**

2.1 Historical Development of Shear Design Provision 6
2.2 Theoretical Background 10
2.2.1 Diagonal tension in homogeneous elastic beams 10
2.2.2 Behavior of beams failing in shear 13
2.2.3 Beam action and Arch action in shear behavior of reinforced concrete members 16
2.2.4 Factors affecting the shear strength of beams without web reinforcement 18
2.2.5 Shear and flexural cracking in reinforced concrete members 21
2.3 Shear Design Models 23
2.3.1 Truss model for design of reinforced concrete structures 23
2.3.2 Compression Field Approaches 30
2.4 Shear design procedures using Modified Compression Field theory 39
2.4.1 Design procedure based on Modified Compression Field Theory 39
2.4.2 Design procedure based on the simplified Modified Compression Field Theory 44
2.5 Building Codes and Shear Design Provisions 46
2.5.1 Overview of current ACI Design Procedures (ACI 318-14) 47
2.5.2 Overview of Recent European Codes (EN 1992:2004) 48

CHAPTER 3 BUILDING CODES AND EFFECT OF SPACING **49**

CHAPTER 4 EXPERIMENTAL PROGRAM 57

4.1 Specimens 57

4.2 Materials 60

4.2.1 Concrete 60

4.2.2 Steel 61

4.3 Specimen Fabrication 63

4.4 Test Setup 64

4.5 Instrumentation 65

CHAPTER 5 FEM ANALYSIS USING DUCOM-COM3 67

5.1 About the software 67

5.2 Specimens 67

5.3 Materials 74

5.4 Modeling 74

5.5 Support condition and loading 75

CHAPTER 6 RESULT AND DISCUSSION 76

6.1 Result from experiment 76

6.1.1 Result 76

6.1.2 Effect of spacing of web reinforcement 79

6.1.3 Effect of arrangement of web reinforcement 79

6.2 Result from finite element analysis using DuCOM-COM3 81

6.2.1 Result 81

6.2.2 Effect of spacing and arrangement of stirrups 83

6.3 Comparison between result from analytical simulation and experiment 83

CHAPTER 7 CONCLUSION AND RECOMMENDATION 87

7.1 Conclusion 87

7.2 Recommendation 87

REFERENCES 89

LIST OF TABLES

Table 2-1 – Values of β and θ for members with at least minimum shear reinforcement....42

Table 2-2 – Values of β and θ for members with less than minimum shear reinforcement.43

Table 3-1 – Comparison of different design approaches....50

Table 3-2 – Code assessment for RC and PC members....55

Table 4-1 – Details of investigated specimens....58

Table 4-2 – 14th day strength of cylinder samples....61

Table 4-3 – 21st day strength of cylinder samples....61

Table 4-4 – Mix proportions of concrete....61

Table 4-5 – Mechanical properties of reinforcement....62

Table 5-1 - Specimens description....67

Table 5-2 – Mechanical property of concrete....74

Table 5-3 – Mechanical property of reinforcement bar....74

LIST OF FIGURES

Figure 2-1 – Shear in homogeneous rectangular beams 11
Figure 2-2 – Stress trajectories in homogeneous rectangular beam 12
Figure 2-3 – Internal forces in a cracked beam without web reinforcements 13
Figure 2-4 – Internal forces in a cracked beam with web reinforcements 15
Figure 2-5 – Distribution of Internal shears in a beam with web reinforcement 16
Figure 2-6 - Effect of a/d ratio on shear capacity of beams 17
Figure 2-7– Effect of reinforcement ratio on shear capacity of beams constructed with normal-weight concrete and without stirrups 19
Figure 2-8 – Effect of beam depth , d, on failure for beams of various sizes 20
Figure 2-9 – Effect of axial loads on inclined shear 21
Figure 2-10 – Truss analogy 23
Figure 2-11 – Construction of an analogous plastic truss 24
Figure 2-12 – Truss model for design 26
Figure 2-13 – Forces in web reinforcements and compression diagonals 27
Figure 2-14 – 45 Degree Truss Model 29
Figure 2-15 – Example of cracked web of beam falling in shear 32
Figure 2-16 – Compression field theory 33
Figure 2-17 – Aspects of Modified Compression Field Theory 36
Figure 2-18 – Comparison of predicted shear strengths of two series of reinforced concrete elements 38
Figure 2-19 – Determination of strains, ε_x , for nonprestressed beam 40
Figure 2-20 – Values of β and θ for members containing at least the minimum amount of web reinforcements 42
Figure 4-1 – Experiment specimens 59
Figure 4-2 - Compressive strength testing machine 60
Figure 4-3 - Tensile Strength testing machine 62
Figure 4-4 - Reinforcement cage of specimen B2 63
Figure 4-5 - Reinforcement cage of Specimen B1 63
Figure 4-6 - Reinforcement cage of specimen B1 inside the formwork 64
Figure 4-7 – 3D sketch for web reinforcement configuration in specimen B3 64

Figure 4-8 – Hydraulic Jack....64
Figure 4-9 - Test Setup....65
Figure 4-10 - Displacement measuring tool....66
Figure 4-11 - Load Cell....66
Figure 4-12 - Data Logger....66
Figure 6-1 – Initiation of diagonal cracks....76
Figure 6-2 – Diagonal tension failure in Specimen B-2....76
Figure 6-3 – Load – Deflection diagram for specimen B1....77
Figure 6-4 – Load – Deflection diagram for specimen B2....78
Figure 6-5 – Load – Deflection diagram for specimen B3....78
Figure 6-6 – Shear opening displacement (width) in spacemen B-1....79
Figure 6-7 – Slip along shear cracks in specimen B-2....80
Figure 6-8 – Load-Deflection diagram for series-A beams....81
Figure 6-9 – Load-Deflection diagram for series-B beams....82
Figure 6-10 – Load-Deflection diagram for series-C beams....82

ABSTRACT

Shear behavior of beams was a major research area for over a century. However due to the fact that this behavior is dictated by different factors, researchers throughout the world have not come into a common understanding of a defined theory for predicting the shear behavior of beams. Spacing and configuration of stirrups has not been given emphasis as one of the factors affecting the shear behavior of beams. In this study, over 12 well-known building codes were examined for their provision of shear capacity calculation. Each of them has the term "spacing" in their provisions. However, in all of this Building Codes, as long as the web reinforcement ratio (area of stirrup/ spacing) is kept the same, altering spacing of stirrups will not result in different shear capacity prediction.

Three shear-critical beam specimens were examined through experiment to study whether or not the shear behavior is affected by spacing and configuration of stirrups and it was observed that the shear capacity increases inversely with spacing of stirrups.

Analytical simulation was attempted using a non-linear 3D finite element tool called DuCOM-COM3 for a series of shear-critical beams with different arrangement of stirrups and different concrete grades.

CHAPTER 1 INTRODUCTION

1.1 General Background

Shear behavior of reinforced concrete beams is a major area of research for more than 100 years. However, a single globally accepted theory like the flexure theory is not yet developed. From the undergone researches, the famous theories such as the truss model and more recently the Modified Compression field theory has been developed. Truss model has been the most widely used method in different building codes for the past many years. The original truss model follows a procedure of drawing a unique truss configuration for every member depending on the arrangement of web reinforcement, the magnitude of the load, the point of application of the load, and the yield capacity of the web reinforcement. Thus, varying the spacing or the configuration of the web reinforcements will change the configuration of the truss which in turn changes the force in the truss members. From this, we can surely say spacing and configuration of web reinforcements was a factor affecting the shear behavior of beams in the original truss method. However, drawing a unique truss model for every member in a structure was tedious for the designer and a more condensed design equations based on the truss method were needed and the simplified truss model came into practice. The simplified truss model was developed by summing-up the truss elements in the original truss model within certain spacing together as one truss member. In doing so, the shear capacity became a factor of the web reinforcement ratio (area of one web reinforcement per spacing). Thus, if one choose to use the simplified truss model; providing a web reinforcement of area ‘A’ at a spacing ‘S’ results similar capacity to providing a web reinforcement of area ‘2A’ at a spacing ‘2S’.

One of the pioneer researchers on the truss method P. Marti noted “*The main advantages of truss models are their transparency and adaptability to arbitrary geometric and loading configurations. Unfortunately, these advantages have been thrust into the background by several recent developments of design equations based on truss models. Such design equations may simplify the treatment of well-defined standard problems, but their applicability is necessarily restricted. Considering the wide variety of real problems, I recommend the direct and consistent application of truss models rather than the further development of design equations”* [**1**]

The modified compression field approach for shear behavior investigation is a recent approach developed by formulating a constitutive relationship for a cracked concrete through several panel tests of concrete under tension and compression [**2**]. This theory has shown nearly accurate correlation between the experimentally tested beams under different conditions and is now among the recent advancements in the shear behavior modeling. The modified compression theory was adopted in the Canadian code and AASHTO LRFD [**3**]. However, like the truss model, some simplifications were made to make it easily adoptable for design purpose and this included expressing the effect of spacing as the effect of web reinforcement ratio. Thus, similar to the simplified truss model, changing the spacing of the web reinforcement will not change the capacity as long as the ratio of web reinforcement is kept the same.

Therefore, it can clearly be seen that the original theories considered spacing as a factor affecting the shear behavior of beams but building code provision on shear capacity calculation made some simplifications to the original theories and one of the effect of this simplification is making the ratio of web reinforcement a factor affecting the capacity instead of spacing of web reinforcement.

An experimental investigation on shear cracking behavior in reinforced concrete beams with shear reinforcement was done by Mohamed Z. *et.al* and they found that the greater web reinforcement spacing leads to the greater diagonal crack spacing, confirming that there is a significant influence of the web reinforcement spacing on the spacing between shear cracks. [**4**]

On the other hand, while retrofitting reinforced concrete beams, the usual practice is drilling the concrete and introducing vertical web reinforcements to add the capacity from the web reinforcements. However, most of the times these web reinforcements are provided vertically down the beam on each face aligned parallel to each other. Therefore, in addition to studying the effect of spacing on shear behavior of beams, this research will also study the effect of staggering these web reinforcements on each face of the beam while retrofitting.

1.2 Significance

The most widely accepted building codes provisions on shear design of reinforced concrete members present spacing and arrangement of web reinforcement as a factor that does not affect the shear behavior as long as the shear reinforcement ratio is kept similar. According to these codes, the designer is free to choose the spacing which results the required capacity while keeping the web reinforcement ratio similar within the provisions of minimum and maximum spacing.

From previous studies [**4**] which were conducted to study correlation between configuration of web reinforcements and cracking, it was found that the crack width and crack spacing of this members were significantly affected. Thus, this research targets to answer the question of whether or not spacing and arrangement of web reinforcements has an effect on the shear behavior of beams. Furthermore if the spacing and configuration of web reinforcements is found to enhance the capacity, results of this research might suggest an improved way of configuring web reinforcements while designing and retrofitting reinforced concrete members.

1.3 Objectives

The main objective of this research is to study whether or not spacing of web reinforcements affect the shear behavior of beams and to observe the extent of this effect.

On the other hand, if spacing and arrangement of web reinforcement is found to be a factor affecting the shear capacity of beams, a better way of configuring web reinforcement for enhancement of shear strength will be recommended.

1.4 Scope

This research will include only normal beams with internal force of flexure and shear. Deep beams, beam-columns, Pre-stressed beams and beams made of high-strength concrete will not be covered in this reference.

1.5 Methodology

The overall process of this research includes literature review, examination of building codes, experimental program and analytical simulation using non-linear finite element modeling.

First the basic shear design theories such as the truss model and modified compression field approaches will be studied and checked if spacing and arrangement of web reinforcement is a factor affecting the shear behavior of beams in this models. Then, the most widely used building codes provisions and their shear design provisions will be reviewed.

After the desk analysis, finite element analysis for different arrangement of web reinforcements using a nonlinear finite element analysis tool called DuCOM-COM3 will be presented. Furthermore, the reliability of the result of the result obtained using the non-linear finite element tool will be verified by conducting an experiment for selected specimens.

CHAPTER 2 LITERATURE REVIEW

2.1 Historical Development of Shear Design Provision [5]

Most codes of practice use sectional methods for design of conventional beams under bending and shear. ACI building Code 318-95M assumes that flexure and shear can be handled separately for the worst combination of flexure and shear at a given section.

In the early 1900s, truss model was used as conceptual tool in the analysis and design of reinforced concrete beams. Ritter (1989) postulated that after a reinforced concrete beam cracks due to diagonal tension stresses, it can be idealized as a parallel chord truss with compression diagonals inclined at 45^0 with respect to the longitudinal axis of the beam. Morsch (1920, 1922) later introduced the use of truss models for torsion. These truss models neglected the contribution of the concrete in tension. Withey (1907, 1908) introduced Ritter's truss model into the American literature and pointed out that this approach gave conservative results when compared with test evidence. This was further confirmed by Talbot (1909) .

Historically, shear design in the United States has included a concrete contribution, V_c, to supplement the 45^0 sectional truss model to reflect test results in beams and slabs with little or no shear reinforcement and to ensure economy in the practical design of such members. ACI Standard Specification No. 23 (1920) permitted an allowable shear stress of $0.025f'_c$, but not more than 0.41 MPa, for beams without web reinforcement, and with longitudinal reinforcement that did not have 'mechanical anchorage.' If the longitudinal reinforcement was anchored with 180^0 hooks or with plates 'rigidly connected' to the bars, the allowable shear stress was increased to $0.03f_c^{'}$ or a maximum of 0.62 MPa. Web reinforcement was designed by the equation

$$A_v f_v = \frac{V's\ \sin\alpha}{jd} \qquad (1)$$

Where

A_v	area of shear reinforcement within distance s
f_v	allowable tensile stress in the shear reinforcement
jd	flexural lever arm

V'	total shear minus $0.02f_c'bjd$ (or $0.03f_c'bjd$ with special anchorage)
b	width of the web
s	spacing of shear steel measured perpendicular to its direction
α	angle of inclination of the web reinforcement with respect to the horizontal axis of the beam.

The limiting value for the allowable shear stresses at service load was $0.06f_c^{'}$ or a maximum of 1.24 MPa, or with anchorage of longitudinal steel $0.12f_c^{'}$ or a maximum of 2.48 MPa. This shear stress was intended to prevent diagonal crushing failures of the web concrete prior to yielding of the web reinforcements. These specifications of the code calculated the nominal shear stress as $\upsilon = V / bjd$.

This procedure, which formed the basis for future ACI codes, lasted from 1921 to 1951, with each edition providing somewhat less conservative design procedures. In 1951 the distinction between members with and without 'mechanical anchorage' was omitted and replaced by the requirement that all plain bars must be hooked, and deformed bars must meet ASTM A 305. Therefore, the maximum allowable shear stress on the concrete for beams without web reinforcement (ACI 318-51) was $0.03f_c^{'}$, and the maximum allowable shear stress for beams with web reinforcement was $0.12f_c^{'}$.

ACI 318-51, based on allowable stresses, specified that web reinforcement must be provided for the excess shear if the shear stress at service loads exceeded $0.03f_c^{'}$. Calculation of the area of shear reinforcement continued to be based on a 45^0 truss analogy in which the web reinforcement must be designed to carry the difference between the total shear and the shear assumed to be carried by the concrete.

The august 1955 shear failure of beams in the warehouse of Wilkins Air Force Depot in Shelby, Ohio, brought into question the traditional ACI shear design procedures. These shear failures, in conjunction with intensified research, clearly indicated that shear and diagonal tension was a complex problem involving many variables and resulted in a return to forgotten fundamentals.

Talbot (1909) pointed out the fallacies of such procedures as early as 1908 in talking about the failure of beams without web reinforcement. Based on 106 beam tests, he concluded that

> *"It will be found that the value of shear stress at failure will vary with the amount of reinforcement, with the relative length of the beam, and with other factors which affect the stiffness of the beam… In beams without web reinforcement, web resistance depends upon the quality and strength of the concrete… The stiffer the beam the larger the vertical stresses which may be developed. Short, deep beams give higher results than long slender ones, and beams with high percentage of reinforcement give higher results than beams with a small amount of metal."*

Unfortunately, Talbot's findings about the influence of the percentage of longitudinal reinforcement and the length-to-depth ratio were not reflected in the design equations until much later. The research triggered by the 1956 Wilkins warehouse failures brought these important concepts back to the forefront.

More recently, several design procedures were developed to economize on the design of the web reinforcement one approach has been to add a concrete contribution term to the shear reinforcement capacity obtained, assuming a 45^0 truss (for example, ACI Building Code 318-95). Another procedure has been the use of a truss with a variable angle of inclination of the diagonals. The inclination of the truss diagonals is allowed to differ from 45^0 within certain limits suggested on the basis of the theory of plasticity. This approach is often referred to as the 'standard truss model with no concrete contribution,' and is explained by the existence of aggregate interlock and dowel forces in the cracks, which allow a lower inclination of the compression diagonals and the further mobilization of the web reinforcement. A combination of the variable-angle truss and a concrete contribution has also been proposed. This procedure has been referred to as the modified truss model approach (CEB 1978; Ramirez and Breen 1991). In this approach, in addition to a variable angle of inclination of the diagonals, the concrete contribution for non prestressed concrete members, the concrete contribution is not considered to vary with the level of shear stress. For prestressed concrete members, the concrete contribution is not considered to vary with the level of stress and is taken as a function of the level of prestress and the stress in the extreme tension fiber.

As mentioned previously, the truss model does not directly account for the components of the shear failure mechanism, such as aggregate interlock and friction, dowel action of the longitudinal steel, and shear carried across uncracked concrete. For prestressed beams, the larger the amount of prestressing is the lower the angle of inclination at first diagonal

cracking. Therefore, depending on the level of compressive stress due to prestress, prestressed concrete beams typically have much lower angles of inclined cracks at failure than nonprestressed beams and hence require smaller amounts of web reinforcements.

Traditionally in North American practice, the additional area of longitudinal tension steel for shear has been provided by extending the bars a distance equal to d beyond the flexural cutoff point. Although adequate for a truss model with 45^0 diagonals, this detailing rule is not adequate for trusses with diagonals inclined at lower angles. The additional longitudinal tension force due to shear can be determined from equilibrium conditions of the truss model as $V\cot\theta$, with θ as the angle of inclination of the truss diagonals. Because the shear stresses are assumed uniformly distributed over the depth of the web, the tension acts at the section mid-depth.

The upper limit of shear strength is established by limiting the stress in the compression diagonals, f_d , to a fraction of the concrete cylinder strength. The concrete in the cracked web of a beam is subjected to diagonal compressive stresses that are parallel or nearly parallel to the inclined cracks. The compressive strength of this concrete must be established so as to prevent web crushing failures. The strength of this concrete is a function of (1) the presence or absence of cracks and the orientation of these cracks; (2) the tensile strain in the transverse direction; and (3) the longitudinal strain in the web.

The pioneering work from Ritter and Morsch received new impetus in the period from the 1960s to the 1980s, and therefore in more recent design codes modified truss models are used. Attention was focused on the truss model with diagonals having a variable angle of inclination as a viable model for shear and torsion in reinforced and prestressed concrete beams (Kupfer 1964; Caflisch *et al*. 1971; Lampert and Thurlimann 1971; Thurlimann *et al*. 1983). Further development of plasticity theories extended the applicability of the model to non-yielding domains (Nielsen Braestrup 1975; Muller 1978; Marti 1980). Schlaich *et al*. (1987) extended the truss model for beams with uniformly inclined diagonals, all parts of the structure in the form of strut-and-tie models (STM). This approach is particularly relevant in regions where the distribution of strains is significantly nonlinear along the depth. Schlaich *et al*. introduced the concept of D and B regions, where, where D stands for discontinuity or disturbed, and B stands for beam or Bernouli. In D regions the distribution of strains is nonlinear, whereas the distribution is linear in B regions. A structural concrete member can

consist entirely of a D region; however, more often D and B regions will exist within the same member or structure. In this case, D regions extend a distance equal to the member depth away from any discontinuity, such as a change in cross section or the presence of concentrated loads. For typical slender members, the portions of the structure or member between D regions are B regions.

By analyzing a truss model consisting of linearly elastic members and neglecting the concrete tensile strength, Kupfer (1964) provided a solution for the inclination of the diagonal cracks. Collins and Mitchell (1980) abandoned the assumption of linear elasticity and developed the compression field theory (CFT) for members subjected to torsion and shear. Based on extensive experimental investigation, Vecchio and Collins (1982,1986) presented the modified compression field theory (MCFT), which included a rationale for determining the tensile stresses in the diagonally cracked concrete. Although the CFT works well with medium to high percentages of transverse reinforcement, the MCFT provides a more realistic assessment for members having a wide range of amount of transverse reinforcement including the case of no web reinforcement. Parallel to these developments of the truss model with variable strut inclinations and the CFT, the last decade also saw the further development of shear friction theory. In addition, a general theory was developed for beams in shear using constitutive laws for friction and by determining the strains and deformations in the web. Because this approach considers the discrete formation of cracks, the crack spacing and crack width must be determined and equilibrium checked along the crack to evaluate the crack-slip mechanism of failure.

2.2 Theoretical Background

2.2.1 Diagonal tension in homogeneous elastic beams [6]

The stresses acting in homogenous beams can be derived from mechanics of elastic materials. Shear stresses

$$\nu = \frac{VQ}{Ib} \tag{2}$$

act at any section in addition to the bending stresses

$$\sigma = \frac{My}{I} \tag{3}$$

except for those locations at which the shear force V happens to be zero.

The role of shear stresses is easily visualized by the performance under load of the laminated beam of Figure 2-1; it consists of two rectangular pieces bonded together along the contact surface. If the adhesive is strong enough, the member will deform as one single beam, as shown in Figure 2-1a . On the other hand, if the adhesive is weak, the two pieces will separate and slide relative to each other, as shown in Figure 2-1b .

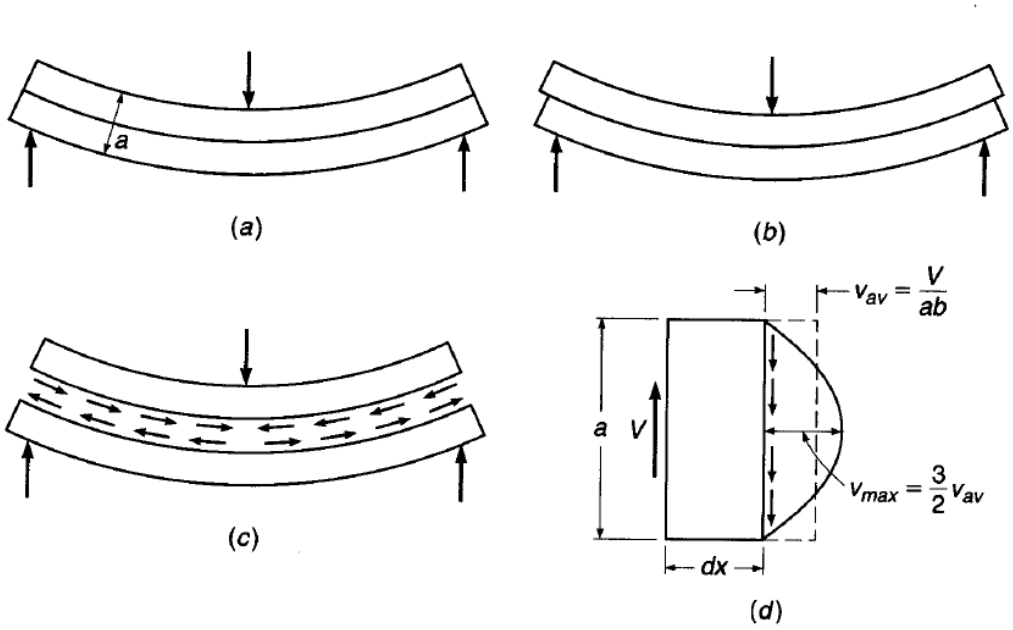


Figure 2-1 – Shear in homogeneous rectangular beams (Arthur H. Nilson *et al.*, 2010)

Evidently, then, when the adhesive is effective, there are forces or stresses acting in it that prevent this sliding or shearing. These horizontal shear stresses are shown in Figure 2-1c as they act, separately, on the top and bottom pieces. The same stresses occur in horizontal planes in single-piece beams; they are different in intensity at different distances from the neutral axis.

Figure 2-1d shows a differential length of a single-piece rectangular beam acted upon by a shear force of magnitude V. Upward translation is prevented; i.e., vertical equilibrium is provided by the vertical shear stresses v . Their average value is equal to the shear force divided by the cross-sectional area $v_{av} = V / ab$, but their intensity varies over the depth of the section. The shear stress is zero at the outer fibers and has a maximum of $1.5v_{av}$ at the neutral axis, the variation being parabolic. If a small square element located at the neutral

axis of such a beam is isolated as shown in Figure 2-2b, the vertical shear stresses on it, equal and opposite on the two faces for reasons of equilibrium, act as shown. However, if these were the only stresses present, the element would not be in equilibrium; it would spin. Therefore, on the two horizontal faces there exist equilibrating horizontal shear stresses of the same magnitude. That is, at any point within the beam, the horizontal shear stresses of Figure 2-2b are equal in magnitude to the vertical shear stresses of Figure 2-1d.

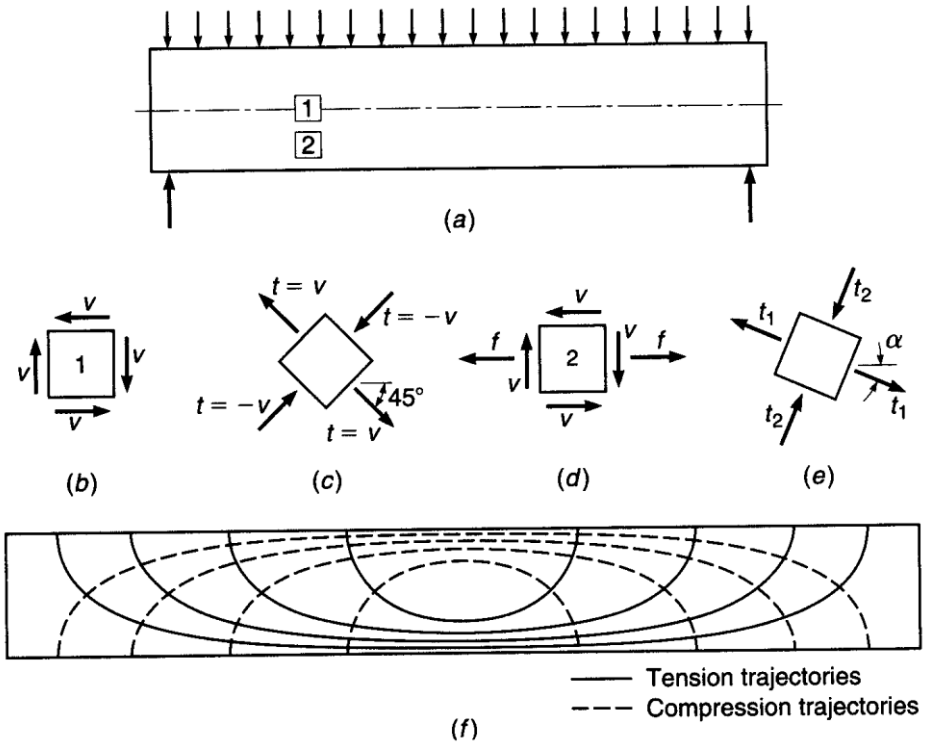


Figure 2-2 – Stress trajectories in homogeneous rectangular beam (Arthur H. Nilson *et al.*, 2010)

It is proved in any strength-of-materials text that on an element cut at 45^0 these shear stresses combine in such a manner that their effect is as shown in Figure 2-2c. That is, the action of the two pairs of shear stresses on the vertical and horizontal faces is the same as that of two pairs of normal stresses, one tensile and one compressive, acting on the 45^0 faces and of numerical value equal to that of the shear stresses. If an element of the beam is considered that is located neither at the neutral axis nor at the outer edges, its vertical faces are subject not only to the shear stresses but also to the familiar bending stresses. The six stresses that now act on the element can again be combined into a pair of inclined compressive stresses and a pair of inclined tensile stresses that act at right angles to each other. They are known as principal stresses (Figure 2-2e).

Since the magnitudes of the shear stresses v and the bending stresses f change both along the beam and vertically with distance from the neutral axis, the inclinations as well as the magnitudes of the resulting principal stresses also vary from one place to another. Figure 2-2f shows the inclinations of these principal stresses for a uniformly loaded rectangular beam. That is, these stress trajectories are lines which, at any point, are drawn in that direction in which the particular principal stress, tension or compression, acts at that point. It is seen that at the neutral axis the principal stresses in a beam are always inclined at 45^0 to the axis. In the vicinity of the outer fibers they are horizontal near midspan.

An important point follows from this discussion. Tensile stresses, which are of particular concern in view of the low tensile strength of the concrete, are not confined to the horizontal bending stresses f that are caused by bending alone. Tensile stresses of various inclinations and magnitudes, resulting from shear alone (at the neutral axis) or from the combined action of shear and bending, exist in all parts of a beam and can impair its integrity if not adequately provided for. It is for this reason that the inclined tensile stresses, known as diagonal tension, must be carefully considered in reinforced concrete design.

2.2.2 Behavior of beams failing in shear [7]

2.2.2.1 Behavior of beams without web reinforcement

The forces transferring shear across an inclined crack in a beam without web reinforcements are illustrated in Figure 2-3.

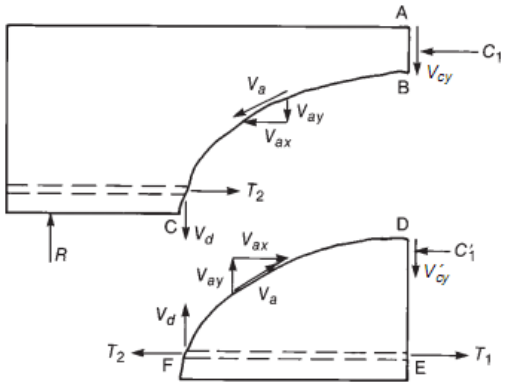


Figure 2-3 – Internal forces in a cracked beam without web reinforcements (McGregor *et al.*, 2012)

Shear is transferred across line A-B-C by V_{cy} , the shear in the compression zone, by V_{ay}, the vertical component of the shear transferred across the crack by interlock of the aggregate particles on the two faces of the crack, and by V_d, the dowel action of the longitudinal reinforcement. Immediately after inclined cracking, as much as 40 to 60 percent of the total shear is carried by V_d and V_{ay} together.

Considering D-E-F portion of the beam below the crack and summing moments about the reinforcement at point E shows that V_d and V_a cause a moment about E that must be equilibrated by a compression force $C_1^{'}$. Horizontal force equilibrium on section A-B-D-E shows that $T_1 = C_1 + C_1^{'}$, and finally, T_1 and $C_1 + C_1^{'}$ must equilibrate the external moment at this section.

As the crack widens, V_a decreases, increasing the fraction of the shear resisted by V_{cy} and V_d . The dowel shear, V_d, leads to a splitting crack in the concrete along the reinforcement. When this crack occurs, V_d drops, approaching zero. When V_a and V_d disappear, so do V_{cy} ' and $C_1^{'}$, with the result that all the shear and compression are transmitted in the depth AB above the crack. At this point in the life of the beam, the section A-B is too shallow to resist the compression forces needed for equilibrium. As a result, this region crushes or buckles upward.

Note also that if $C_1^{'} = 0$, then $T_2 = T_1$, and as a result, $T_2 = C_1$. In other words, the inclined crack has made the tensile force at point C a function for the moment at section A-B-D-E. This shift in the tensile force must be considered in detailing the bar cut off points and in anchoring the bars.

2.2.2.2 Behavior of beams with web reinforcement

Inclined cracking causes the shear strength of beams to drop below the flexural capacity. The purpose of web reinforcement is to ensure that the full flexural capacity can be developed.

Prior to inclined cracking, the strain in the web reinforcement is equal to the corresponding strain of the concrete. Because concrete cracks at a very small strain, the stress in the web reinforcements prior to inclined cracking will not exceed 3 to 6 ksi. Thus, web reinforcements

do not prevent inclined cracks from forming; they come into play after the cracks have formed.

The forces in a beam with web reinforcements and an inclined crack are shown in Figure 2-4.

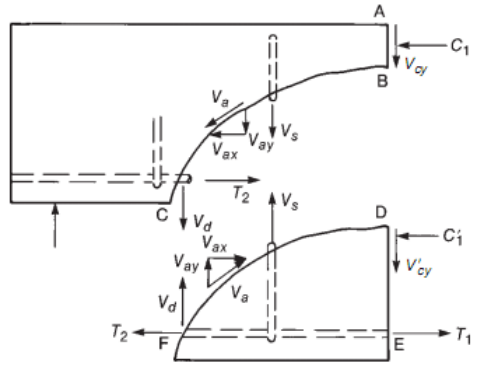


Figure 2-4 – Internal forces in a cracked beam with web reinforcements (McGregor *et al.*, 2012)

The shear transferred by tension in the web reinforcements, V_s , does not disappear when the crack opens wider, so there will always be a compression force C_1' and a shear force V_{cy}' acting on the part of the beam below the crack. As a result, T_2 will be less than T_1 , the difference depending on the amount of web reinforcement. The force T_2 will however, be larger than the flexural tension $T = M / jd$ based on the moment at C.

The loading history of such a beam is shown qualitatively in Figure 2-5.

The components of the internal shear resistance must equal the applied shear, indicated by the upper 45^0 line. Prior to flexural cracking, the entire shear is carried by the uncracked concrete. Between flexural and inclined cracking, the external shear is resisted by V_{cy} , V_{ay}, and V_d. Eventually, the web reinforcements crossing the crack yield, and V_s stays constant for higher applied shears. Once the web reinforcements yield, the inclined crack opens more rapidly. As the inclined crack widens, V_{ay} decreases further, forcing V_d and V_{cy} to increase at an accelerated rate, until either a splitting (dowel) failure occurs, the compression zone crushes due to combined shear and compression, or the web crushes.

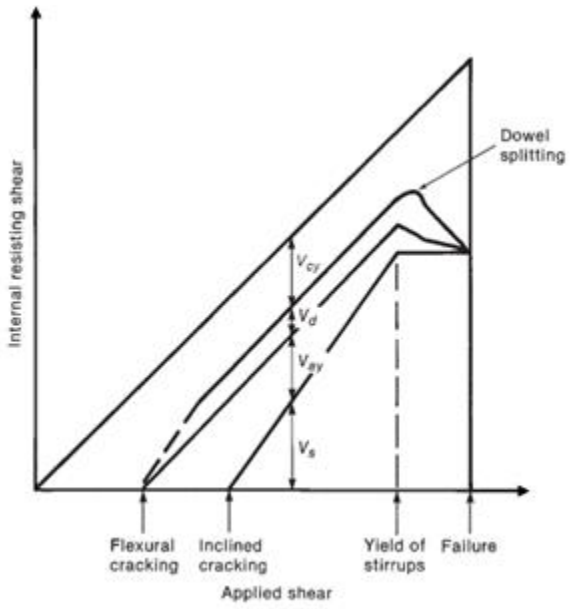


Figure 2-5 – Distribution of Internal shears in a beam with web reinforcement (McGregor *et al.*, 2012)

Each of the components of this process except V_s has a brittle load-deflection response. As a result, it is difficult to quantify the contributions of V_{cy}, V_d, and V_{ay}. In design, these are lumped together as V_c, referred to somewhat incorrectly as "the shear carried by the concrete." Thus, the nominal shear strength, V_n, is assumed to be

$$V_n = V_c + V_s \tag{4}$$

2.2.3 Beam action and Arch action in shear behavior of reinforced concrete members [7]

The behavior of beams failing in shear varies widely, depending on the relative contributions of beam action and arch action and the amount of web reinforcement.

The moments and shear at inclined cracking and failure of rectangular beams without web reinforcement are plotted in the Figure 2-6 as a function of the ratio of the shear span **a** to the depth **d**.

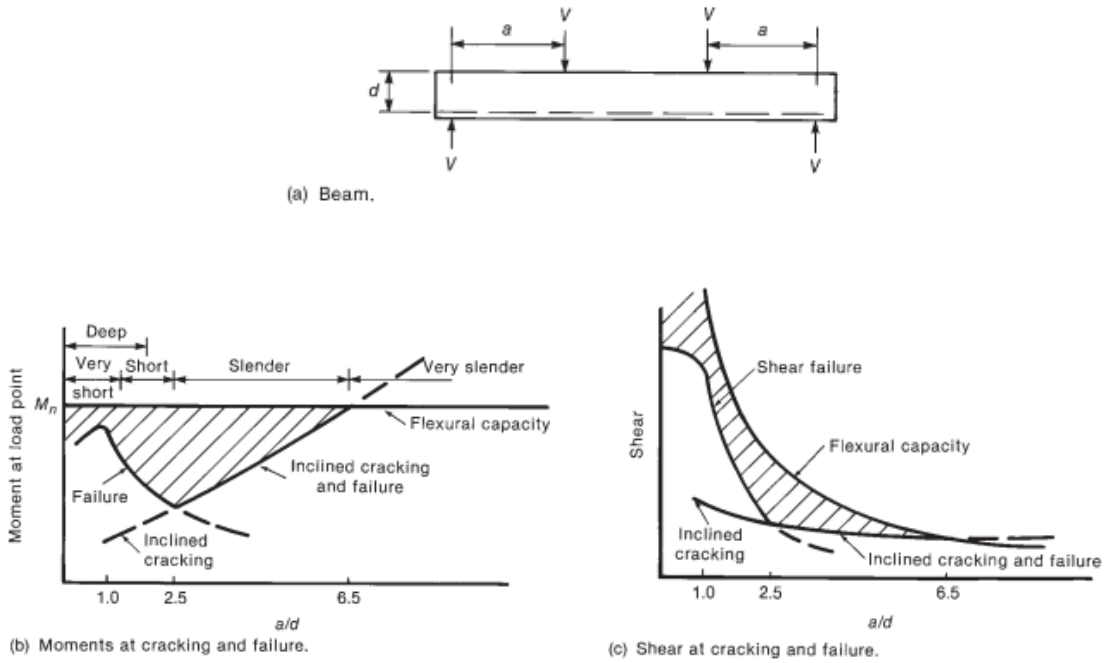


Figure 2-6 - Effect of a/d ratio on shear capacity of beams (McGregor *et al.*, 2012)

The beam cross section remains constant as the span is varied. The maximum moment capacity, M_n , of the cross section plotted as a horizontal line in Figure b. The shaded areas in this figure show the reduction in strength due to shear. Web reinforcement is normally provided to ensure that the beam reaches the full flexural capacity, M_n .

The figure suggests that the shear spans can be divided into three types: short, slender, and very slender shear spans. The term deep beam is also used to describe beams with short shear spans. Very short shear spans, with a/d from 0 to 1, develop inclined cracks joining the load and the support. These cracks, in effect, destroy the horizontal shear flow from the longitudinal steel to the compression zone, and the behavior changes from beam action to arch action. Here, the reinforcement serves as the tension tie of a tied arch and has a uniform tensile force from support to support. The most common mode of failure in such beams is an anchorage failure at the ends of the tension tie.

Short shear spans with a/d from 1 to 2.5 develop inclined cracks and, after a redistribution of internal forces, are able to carry additional load, in part by arch action. The final failure of such beams will be caused by bond failure, a splitting failure, or a dowel failure along the tension reinforcement or by crushing of the compression zone over the top of the crack. The latter is referred to as a shear compression failure. Because the inclined crack generally

extends higher into the beam than does a flexural crack, failure occurs at less than the flexural moment capacity.

In slender shear spans, those having a/d from about 2.5 to about 6, the inclined cracks disrupt equilibrium to such an extent that the beam fails at the inclined cracking load. Very slender beams, with a/d greater than about 6, will fail in flexure prior to the formation of inclined cracks.

It is important to note that, for short and very short beams, a major portion of the load capacity after inclined cracking is due to load transfer by the compression struts. If the beam is not loaded on the top and supported on the bottom, these compression struts will not form and failure occurs at, or close to the inclined cracking load.

Because the moment at the point where the load is applied is $M = Va$ for a beam loaded with concentrated loads. Figure b can be replotted in terms of shear capacity. The shear corresponding to a flexural failure is the upper curved line. If web reinforcements are not provided, the beam will fail at the shear given by the "shear failure" line. This is roughly constant for a/d greater than about 2. Again, the shaded area indicates the loss in capacity due to shear. Note that the inclined cracking loads of the short shear spans and slender shear spans are roughly constant. This is recognized in design by ignoring a/d in the equations for the shear at inclined cracking. In case of slender beams, inclined cracking causes an immediate shear failure if no web reinforcement is provided.

2.2.4 Factors affecting the shear strength of beams without web reinforcement [7]

Beams without web reinforcement will fail when inclined cracking occurs or shortly afterwards. For this reason, the shear capacity of such members is taken equal to the inclined cracking shear. The inclined cracking load of a beam is affected by five principal variables, some included in design equations and others not.

- Tensile strength of concrete

The inclined cracking load is a function of the tensile strength of the concrete, f_{ct}. The stress state in the web of the beam involves biaxial principal tension and compression stresses. A similar biaxial state of stress exists in a split-cylinder tension test, and the inclined cracking load is frequently related to the strength from such a test. As discussed earlier, the flexural

cracking that precedes the inclined cracking disrupts the elastic-stress field to such an extent that inclined cracking occurs at a principal tensile stress roughly half of f_{ct} for the uncracked section.

- Longitudinal reinforcement ratio, ρ_w

When the steel ratio, ρ_w, is small, flexural cracks extend higher into the beam and open wider than would be the case for large values of ρ_w. And increase in crack width causes a decrease in the maximum values of the components of shear, V_d and V_{ay}, that are transferred across the inclined cracks by dowel action or by shear stresses on the crack surfaces. Eventually, the resistance along the crack drops below that required to resist the loads, and the beam fails suddenly in shear.

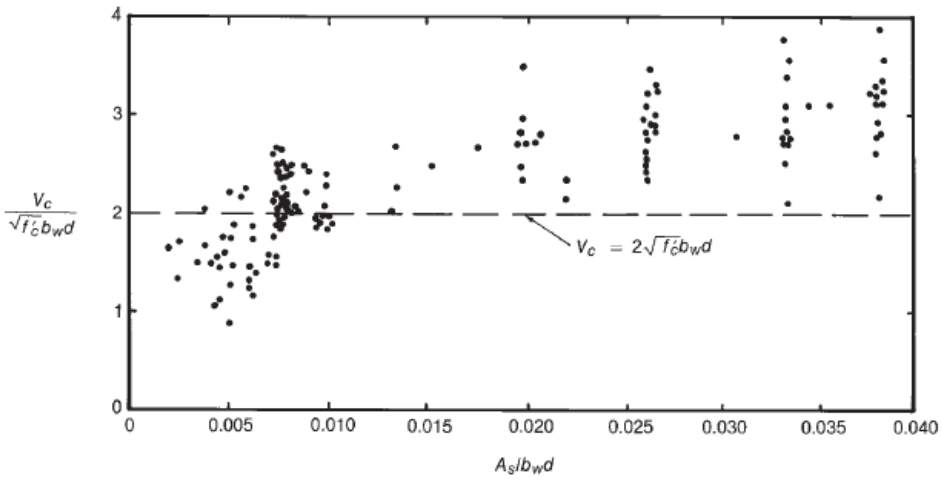


Figure 2-7– Effect of reinforcement ratio on shear capacity of beams constructed with normal-weight concrete and without stirrups (McGregor *et al*., 2012)

- Shear span to depth ratio, a/d

The shear span to depth ratio ,a/d or MV/d, affects the inclined cracking shears and ultimate shears of portions of members with a/d less than 2.

- Lightweight aggregate concrete

Lightweight aggregate concrete has a lower tensile strength than normal weight concrete for a given concrete compressive strength. Because the shear strength of a concrete member

without shear reinforcement is directly related to the tensile strength of a concrete, equations for shear capacity must be modified for members constructed with light weight concrete.

- Size of beam

An increase in the overall depth of a beam with very little (or no) web reinforcement results in a decrease in the shear at failure for a given f_c' , ρ_w , and a/d. The width of an inclined crack depends on the product of the strain in the reinforcement crossing the crack and the spacing of the cracks. With increasing beam depth, the crack spacings and the crack widths tend to increase. This leads to a reduction in the maximum shear stress that can be transferred across the crack by aggregate interlock. An unstable situation develops when the shear stresses transferred across the crack exceeds the shear strength. When this occurs, the faces of the crack slip, one relative to the other.

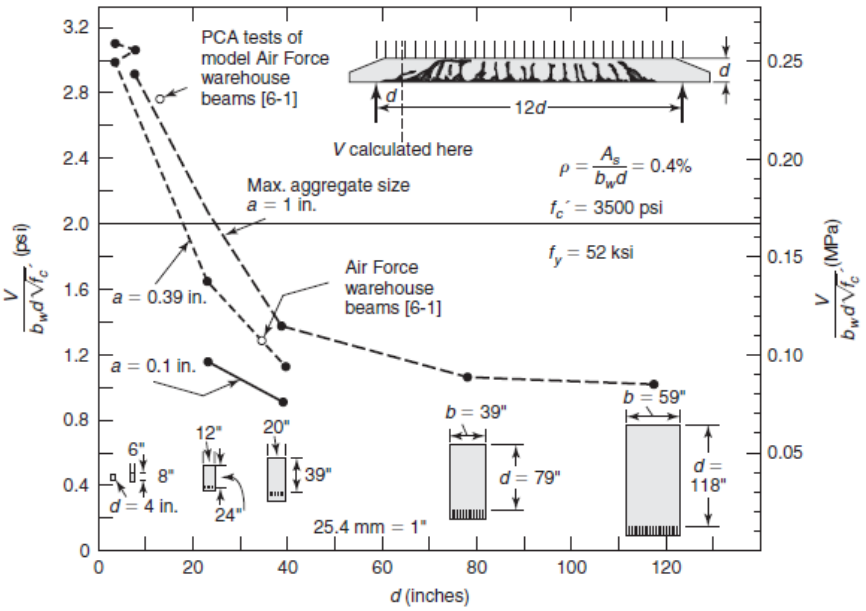


Figure 2-8 – Effect of beam depth , d, on failure for beams of various sizes (McGregor *et al.*, 2012)

- Axial forces

Axial tensile forces tend to decrease the inclined cracking load, while axial compressive forces tend to increase it. As the axial compressive force is increased, the onset of flexural cracking is delayed, and the flexural cracks do not penetrate as far into the beam. Axial tension forces directly increase the tension stress, and hence the strain, in the longitudinal

reinforcement. This causes an increase in the inclined crack width, which, in turn, results in a decrease in the maximum shear tension stress that can be transmitted across the crack. This reduces the shear failure load.

A similar increase is observed in prestressed concrete beams. The compression due to prestressing reduces the longitudinal strain, leading to a higher failure load.

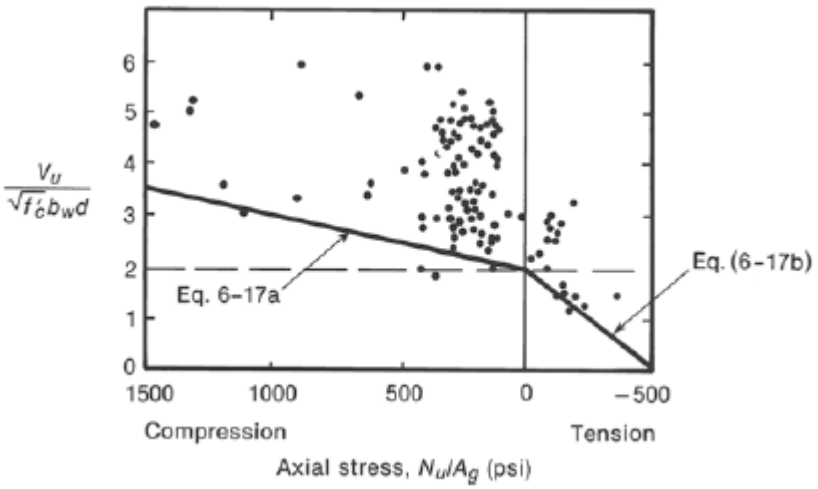


Figure 2-9 – Effect of axial loads on inclined shear (McGregor *et al.*, 2012)

- Coarse aggregate size

As the size (diameter) of the coarse aggregate increases, the roughness of the crack surfaces increases, allowing higher shear stresses to be transferred across the cracks. In high strength concrete beams and some light weight concrete beams, the cracks penetrate pieces of the aggregate rather than going around them, resulting in a smoother crack surface. This decrease in the shear transferred by aggregate interlock along the cracks reduces V_c .

2.2.5 Shear and flexural cracking in reinforced concrete members [4]

Generally, the control of cracking in concrete structures is a desirable matter to satisfy durability and serviceability requirements. In the available literature, many investigations in regard to tensile and fexural cracks for RC members were conducted during last decades (Broms 1965; Clark 1956; Gergely and Lutz 1968), but for shear cracks much concern should be given. The aim of this section is to show the main differences between shear cracking mechanism and flexural cracking mechanism in RC members.

As matter of fact, shear crack opening displacements (or width) in RC members are usually accompanied by shear crack sliding displacements (or slip) along shear cracks which create shear transferred by aggregate interlock. Shear sliding displacement (slip) which is related to shear opening displacement (width) is a main factor for fracturing of shear reinforcement, especially under cyclic loading. Conversely, in the regions of constant bending moment only tensile and flexural crack width occur without sliding along the crack.

In further studies (Hassan and Ueda 1987; Hassan *et al*.1991), it was reported that shear crack opening displacements are not only produced by elongation of vertical leg of web reinforcement, but also are affected by slip of web reinforcement hooks and elongation of horizontal leg of web reinforcement which cause slip at the web reinforcement bent portion. However, flexural crack opening is usually produced by elongation of tension reinforcing bars only since there is no slip at their end.

Furthermore, it was observed in a previous study carried by Hassan and Ueda (1987) that diagonal crack spacings are not significantly affected by the type of shear reinforcing bars (plain or deformed). However, many investigations reported that the spacing between flexural cracks is influenced by the type of reinforcing bars. In addition, shear crack opening displacements are affected by the angle between the shear reinforcement and shear cracks. Greater shear crack widths were found in the beams with vertical web reinforcements rather than with inclined web reinforcements at the same web reinforcement strain (Hassan *et al*. 1985). A shear crack generally crosses shear and tension reinforcement diagonally, while a flexural crack intersects perpendicularly main longitudinal reinforcement.

It was noticed previously (Gergely and Lutz 1968) that the flexural crack width was found to vary directly with the distance from the nearby bar. Broms (1965) stated that the widths of the primary tensile cracks close to the reinforcement were found to be considerably less than the crack widths at the surface of flexural members. It was also proved in the current study that there is a significant effect of the side concrete cover to web reinforcement on shear crack width at the surface of RC members. Shear crack with varies directly with the distance from the nearby web reinforcement due to the bond between the web reinforcement and the surrounding concrete. This result coincides with the concepts of flexural cracks mechanism.

2.3 Shear Design Models

2.3.1 Truss model for design of reinforced concrete structures

The behavior of beams failing in shear must be expressed in terms of a mechanical mathematical model before designers can make use of this knowledge in design. MacGregor *et al*. once stated that the best model for beams with web reinforcement is the truss model. However with the current advances[1] in models for the shear design of reinforced concrete the statement once made by MacGregor can merely be true.

In 1899 and 1902, respectively, the Swiss engineer Ritter and the German engineer Morch, independently, published papers proposing the truss analogy for the design of reinforced concrete beams for shear. These procedures provide an excellent conceptual model to show the forces that exist in a cracked concrete beam. [**7**]

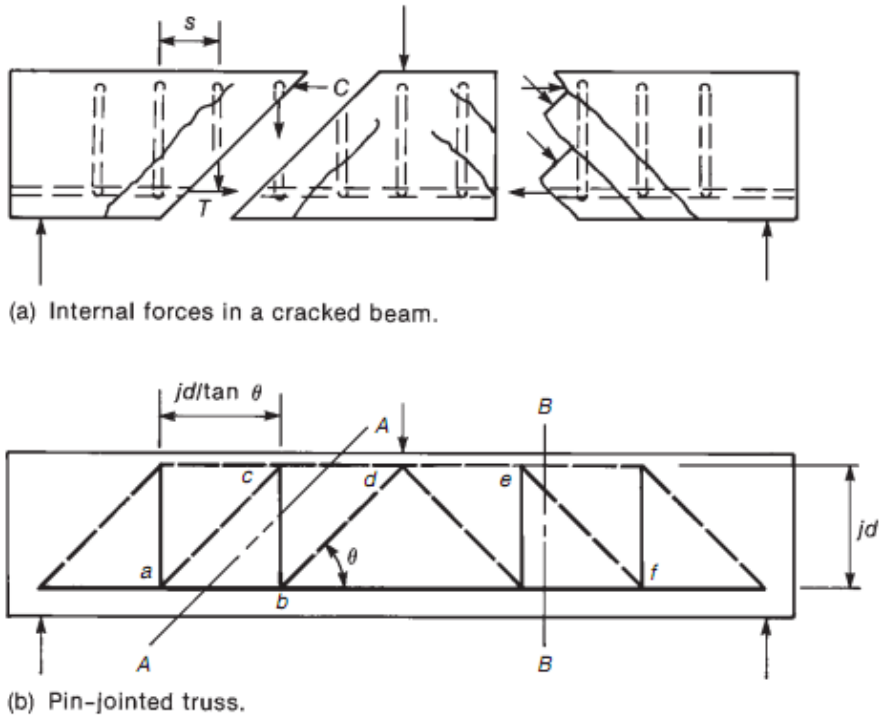


Figure 2-10 – Truss analogy (MacGregor *et al*., 2012)

As shown in Figure 2-10, a beam with inclined cracks develops compressive and tensile forces, C and T, in its top and bottom "flanges," vertical tensions in the web reinforcements,

[1] Compression Field Theory (CFT) and Modified Compression Theory (MCFT)

and inclined compressive forces in the concrete "diagonals" between the inclined cracks. This highly indeterminate system of forces can be replaced by an analogous truss. The simplest truss is shown in Figure 2-10b; a more complicated truss is shown in Figure 2-11b.

Several assumptions and simplifications are needed to derive the analogous truss. In Figure 2-10b, the truss has been formed by lumping all of the web reinforcements cut by section A-A into one vertical member b-c and all the diagonal concrete members cut by section B-B into one diagonal member e-f. This diagonal member is stressed in compression to resist the shear on section B-B. The compression chord along the top of the truss is actually a force in the concrete but is shown as a truss member. The compressive members in the truss are shown with dashed lines to imply that they are really forces in the concrete, not separate truss members. The tensile members are shown with solid lines.

Figure 2-11a shows a beam with inclined cracks. The left end of this beam can be replaced by the truss shown in Figure 2-11b.

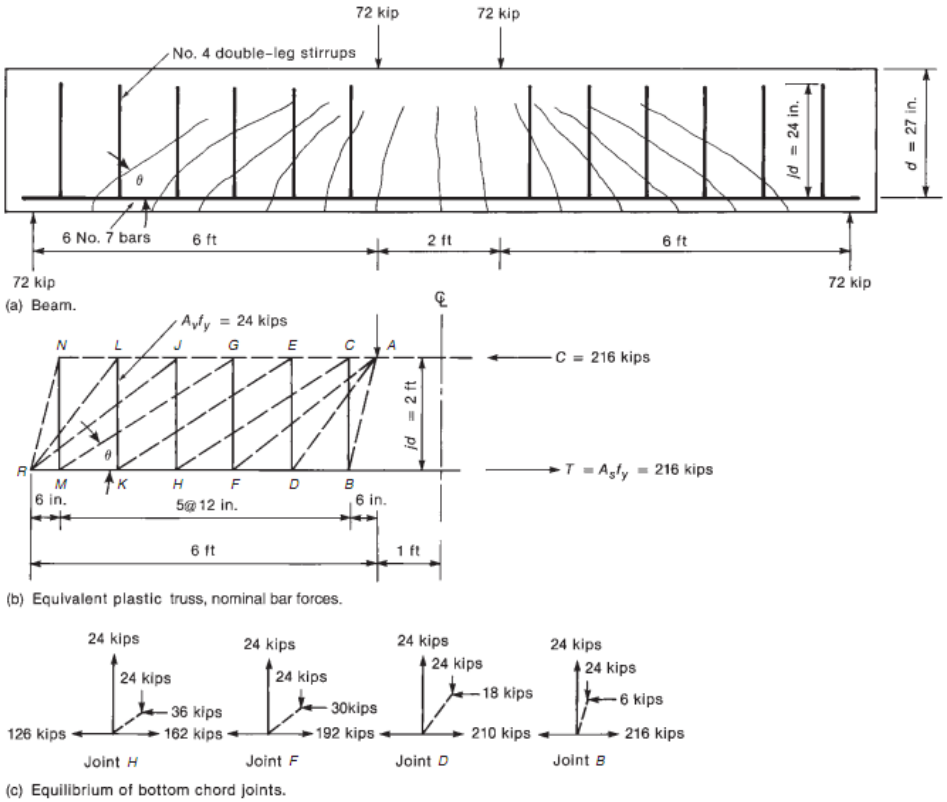


Figure 2-11 – Construction of an analogous plastic truss (MacGregor *et al.*, 2012)

In design, the ideal distribution of web reinforcements would correspond to all web reinforcements reaching yield by the time the failure load is reached. It will be assumed, therefore, that all the web reinforcements have yielded and that each transmits a force of $A_v f_{yt}$ across the crack, where A_v is the area of the web reinforcement legs and f_{yt} is the yield strength of the transverse reinforcement. When this is done, the truss becomes statically determinate. This truss is referred to as a plastic-truss model, because we are depending on plasticity in the web reinforcements to make it statically determinate. The beam will be proportioned so that the web reinforcements yield before the concrete crushes, so that it will not depend on plastic action in the concrete.

This truss model ignores the shear components V_{cy}, V_d, and V_{ay}. Thus it does not assign any shear "to the concrete."

The compression diagonals originating at the load point A (AB, AD, and AF) are referred to as a compression fan. The number of diagonal struts in the fan must be such that the entire vertical load at A is resisted by the vertical force components in the diagonals meeting at A. A similar compression fan exists at the support R (RN, RL, and RJ). Between the compression fans is a compression field consisting of the parallel diagonal struts CH, EK, and KM. The angle θ of the compression field is determined by the number of web reinforcements needed to equilibrate the vertical loads in the fans.

Each of the compression fans occurs in a D-region (discontinuity region). The compression field is a B-region (beam region)

2.3.1.1 Simplified Truss analogy [7]

A statically determinate truss analogy can be derived via the method suggested by Marti. Figure 2-12a and b show a uniformly loaded beam with web reinforcements and a truss model incorporating all the web reinforcements and representing the uniform load as a series of concentrated loads at the panel points. This truss in Figure 2-12b is statically indeterminate, but it can be solved if it is assumed that the forces in each web reinforcement cause the web reinforcement to just reach yield.

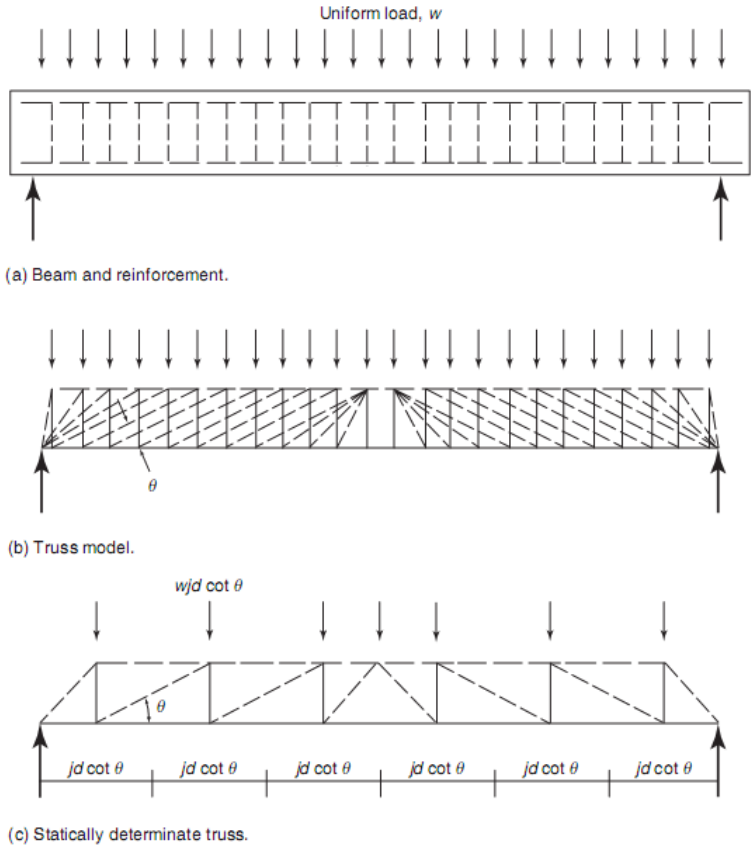


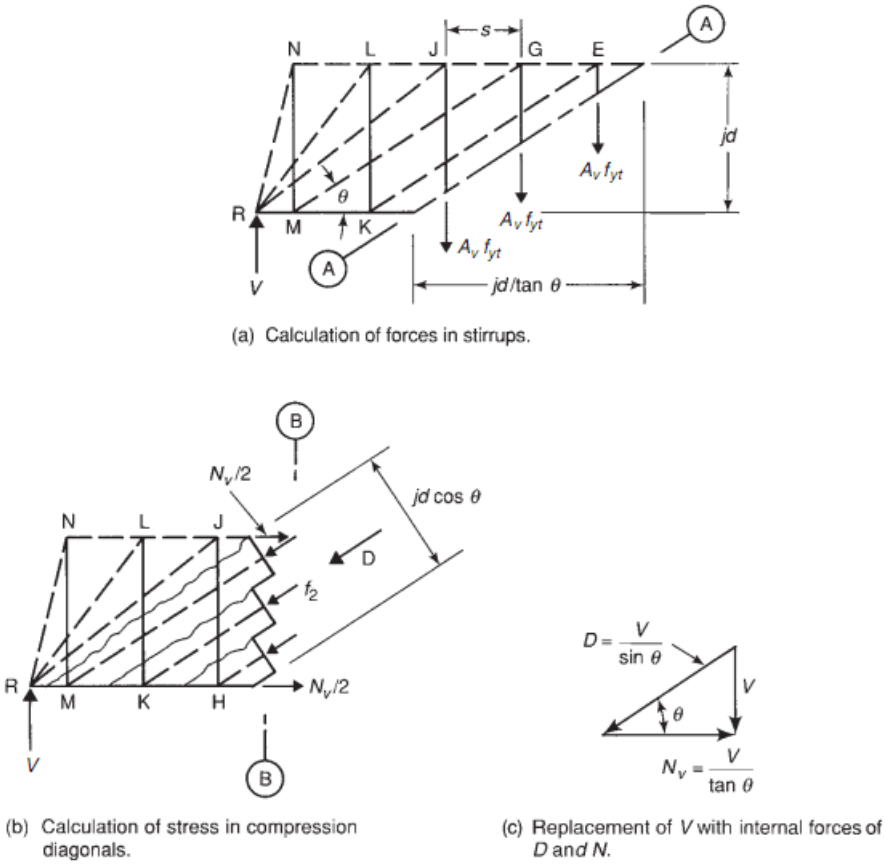
Figure 2-12 – Truss model for design (McGregor *et al.*, 2012)

For design, it is easier to represent the truss as shown in Figure 2-12c, where the tension force in each vertical member represents the force in all the web reinforcements within a length $jd\cot\theta$. Similarly, each inclined compression strut represents a width of web equal to $jd\cos\theta$. The uniform load has been idealized as concentrated loads of $w\left(jd\cot\theta\right)$ acting at the panel points. This truss is statically determinate. To draw such a truss, it is necessary to choose θ.

Internal Forces in the Plastic-Truss Model

If we consider the free-body diagram cut by section A-A parallel to the diagonals in the compression field region in Figure 2-13a, the entire vertical component of the shear force is resisted by tension forces in the web reinforcements crossing this section. The horizontal projection of section A-A is $jd\cot\theta$, and the number of web reinforcements it cuts is $jd\cot\theta / s$. The force in one web reinforcement is $A_v f_{yt}$, which can be calculated from

$$A_v f_{yt} = \frac{V \times s}{jd \cot\theta} \tag{5}$$



(a) Calculation of forces in stirrups.

(b) Calculation of stress in compression diagonals.

(c) Replacement of *V* with internal forces of *D* and *N*.

Figure 2-13 – Forces in web reinforcements and compression diagonals (McGregor *et al*., 2012)

The free body shown in Figure 2-13b is cut by a vertical section between G and J in Figure 2-11b. Here, the vertical force, V, acting on the section is resisted by the vertical component of the diagonal compressive force D (Figure 2-13c). The width of the diagonals is $jd\cos\theta$, as shown in Figure 2-13b, and expressing D as $V/\sin\theta$, the average compressive stress in the diagonals is

$$f_2 = \frac{V}{b_w jd \cos\theta \sin\theta} \tag{6}$$

With the use of trigonometric identities, this equation becomes

$$f_2 = \frac{V}{b_w jd}\left(\tan\theta + \frac{1}{\tan\theta}\right) \tag{7}$$

Where b_w is the thickness of the web. If the web is very thin, this stress may cause the web to crush.

The shear V on section B-B of Figure 2-13b can be replaced by the diagonal compression force

$$D = \frac{V}{\sin\theta} \tag{8}$$

And an axial tension force

$$N_v = \frac{V}{\tan\theta} \tag{9}$$

as shown in Figure 2-13c.

If it is assumed that the shear stress is constant over the height of the beam, the resultants of D and N_v act at mid height. As a result, a tensile force of $N_v/2$ acts in each of the top and bottom chords. This reduces the force in the compression chord and increases the force in the tension chord.

Value of θ in Compression Field Region

When a reinforced concrete beam with web reinforcements is loaded to failure, inclined cracks initially develop at an angle of 35 to 45^0 with the horizontal. With further loading, the angle of the compression stresses may cross some of the cracks. For this to occur, aggregate interlock must exist.

The allowable range of θ is expressed as $0.5 \le \cot\theta \le 2.0$ (θ =26 to 64^0) in the Swiss code. This range was selected to limit crack widths. A more restricted range, $\frac{3}{5} \le \cot\theta \le \frac{5}{3}$ (θ =31 to 59^0), is allowed in the FIP Design Recommendations.

In design, the value of θ should be in the range $25^0 \le \theta \le 65^0$. The choice of a small value of θ reduces the number of web reinforcements required, but increases the compression stresses in the web and increases N_v . The opposite is true for large angles.

In the analysis of a given beam, the angle θ is determined by the number of web reinforcements needed to equilibrate the applied loads and reactions. The angle should be within the limits given, except in compression-fan regions where the angle θ varies. In the design of a beam, the crack angle is a free choice that leads to values of the other unknowns.

Crushing Strength of Concrete in the Web

The web of the beam will crush if the inclined compressive stress, f_2 from , exceeds the strength of the concrete. The compressive strength, f_{2max} , of the concrete in a web that has previously been cracked and that contains web reinforcements stressed in tension at an angle to the cracks will tend to be less than $f_c^{'}$. A reasonable limit is $0.25f_c^{'}$ for $\theta = 30^0$, increasing to $0.45f_c^{'}$ for $\theta = 45^0$.

2.3.1.2 Traditional 45 – Degree Truss Model [8]

Formation of the 45-Degree Truss

Figure 2-14 shows a truss model for a simple beam in which the directions of the diagonal compression stresses are assumed to remain 45 degrees. This truss model of a cracked reinforced concrete beam can be formed by:

- Lumping all of the web reinforcements cut by section A-A into one vertical member.
- Lumping the diagonal concrete members cut by section B-B into one diagonal member with an angle of inclination of 45^0 with respect to the beam axis. This diagonal member is stressed in compression to resist the shear on section B-B.
- Considering the longitudinal tension reinforcement as the bottom chord of the truss.
- Considering the flexural compression zone of the beam acts as the top chord.

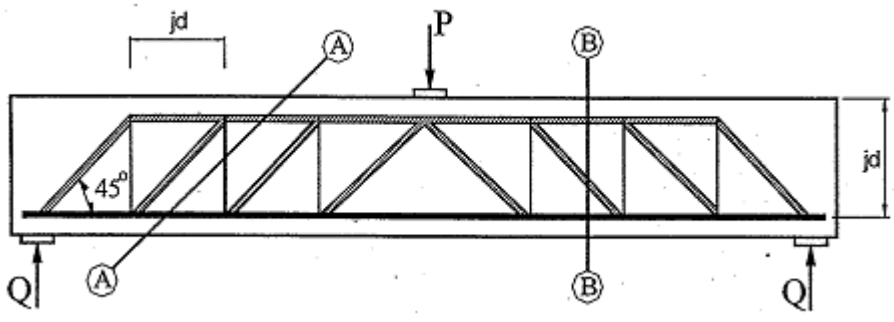


Figure 2-14 – 45 Degree Truss Model (Mahmoud El-Mihilmy *et al*., 2008)

Internal Forces in the 45 Degree Truss Model

Internal forces in the 45 degree truss model can easily be found by substituting 45 degree for the value of θ in the equations derived for the variable angle truss analogy. Thus substituting for the value of θ results the force in each web reinforcement, diagonal compressive force in the concrete and additional tensile and compressive forces at the upper and bottom of the truss chord as follows.

$$A_v f_{yt} = \frac{V \times s}{jd} \quad (10)$$

$$f_2 = \frac{V}{0.5 b_w jd} \quad (11)$$

$$D = \frac{V}{\sin 45} \quad (12)$$

$$N_v = V \quad (13)$$

2.3.2 Compression Field Approaches [5]

2.3.2.1 Introduction

The cracked web of a reinforced concrete beam transmits shear in a relatively complex manner. As the load is increased, new cracks form while preexisting cracks spread and change inclination. Because the section resists moment as well as shear, the longitudinal strains and the crack inclinations vary over the depth of the beam.

The early truss models of Ritter (1899) and Morsch (1920,1922) approximated this behavior by neglecting tensile stresses in the diagonally cracked concrete and by assuming that the shear would be carried by diagonal compressive stresses in the concrete, inclined at 45^0 to the longitudinal axis. The diagonal compressive concrete stresses push apart the top and bottom faces of the beam, while the tensile stresses in the web reinforcements pull them together. Equilibrium requires that these two effects be equal. According to the 45^0 truss model, the shear capacity is reached when the web reinforcements yield and will correspond to a shear stress of

$$\upsilon = \frac{A_v f_y}{b_w s} = \rho_v f_y \quad (14)$$

For the beam shown in Figure 2-15, this equation would predict a maximum shear stress of only 0.80 MPa. As the beam actually resisted a shear stress of about 2.38 MPa, it can be seen that the 45^0 truss equation can be very conservative.

One reason why the 45^0 truss equation is often very conservative is that the angle of inclination of the diagonal compressive stresses measured from the longitudinal axis, θ, is typically less than 45^0. The general form of the above equation is

$$\upsilon = \rho_v f_y \cot\theta \qquad (15)$$

With this equation, the strength of the beam shown in Figure 2-15 could be explained if θ was taken equal to 18.60. Most of the inclined cracks shown in Figure 2-15 are not this flat.

Before the general truss equation can be used to determine the shear capacity of a given beam, or to design the web reinforcements to resist a given shear, it is necessary to know the angle θ. Discussing this problem, Morsch (1922) stated, "it is absolutely impossible to mathematically determine the slope of the secondary inclined cracks according to which one can design the web reinforcements." Just seven years after Morsch made this statement, another German engineer, H.A. Wagner (1929), solved an analogous problem while dealing with the shear design of "stressed-skin" aircraft. Wagner assumed that after the thin metal skin buckled, it could continue to carry shear by a field of diagonal tension, provided that it was stiffened by transverse frames and longitudinal stringers. To determine the angle of inclination of the diagonal tension, Wagner considered the deformations of the system. He assumed that the angle of inclination of the diagonal tensile stresses in the buckled thin metal skin would coincide with the angle of inclination of the principal tensile strain as determined from the deformations of the skin, the transverse frames, and the longitudinal stringers. This approach became known as the tension field theory.

Shear design procedures for reinforced concrete that, like the tension field theory, determine the angle θ by considering the deformations of the transverse reinforcement, the longitudinal reinforcement, and the diagonally stressed concrete have become known as compression field approaches. With these methods, equilibrium conditions, compatibility conditions, and stress-strain relationships for both the reinforcement and the diagonally cracked concrete are used to predict the load-deformation response of a section subjected to shear.

Kupfer (1964) and Baumann (1972) presented approaches for determining the angle θ assuming that the cracked concrete and the reinforcement were linearly elastic. Methods for determining θ applicable over the full loading range and based on Wagner's procedure were developed by Collins and Mitchell (1974) for members in torsion, and were applied to shear design by Collins (1978). This procedure was called the compression field theory (CFT).

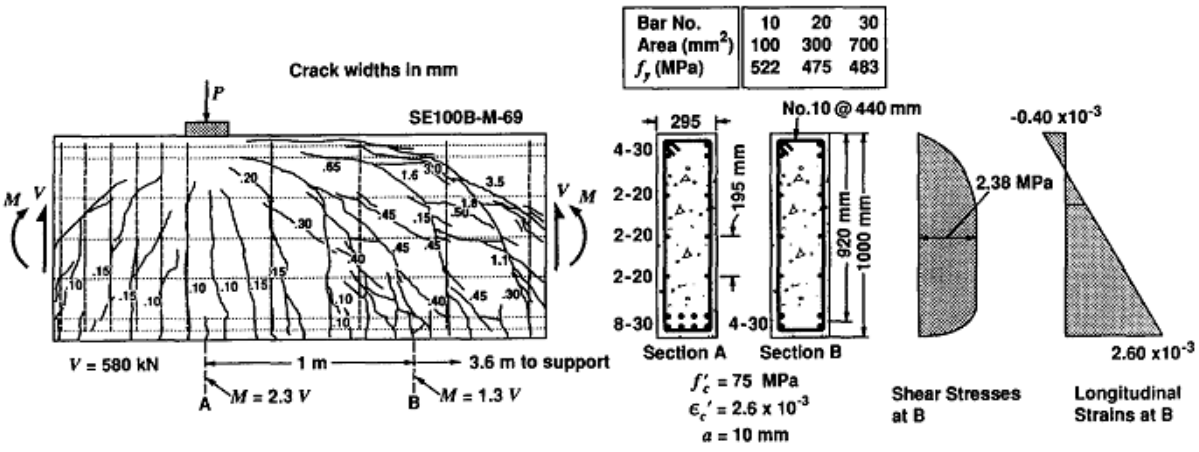


Figure 2-15 – Example of cracked web of beam falling in shear

(ASCE-ACI Commitee 445,1998)

2.3.2.2 Compression Field Theory

Figure 2-16 summarizes the basic relationships of the CFT.

The shear stress, ν, applied to the cracked reinforced concrete causes tensile stresses in the longitudinal reinforcement, f_{sx} , and the transverse reinforcement, f_{sy}, and a compressive stress in the cracked concrete, f_2 , inclined at angle θ to the longitudinal axis. The equilibrium relationships between these stresses can be derived from Figure 2-16(a and b) as

$$\rho_v f_{sy} = f_{cy} = \upsilon \tan\theta \quad (16)$$

$$\rho_x f_{sx} = f_{cx} = \upsilon \cot\theta \quad (17)$$

$$f_2 = \upsilon\left(\tan\theta + \cot\theta\right) \quad (18)$$

Where ρ_x and ρ_v are the reinforcement ratios in the longitudinal and transverse directions.

If the longitudinal reinforcement elongates by a strain of ε_x , the transverse reinforcement elongates by ε_y, and the diagonally compressed concrete shortens by ε_2, then the direction

of principal compressive strain can be found from Wagner's (1929) equation, which can be derived from Mohr's circle of strain [Figure 2-16(d)] as

$$\tan^2\theta = \frac{\varepsilon_x + \varepsilon_2}{\varepsilon_y + \varepsilon_2} \tag{19}$$

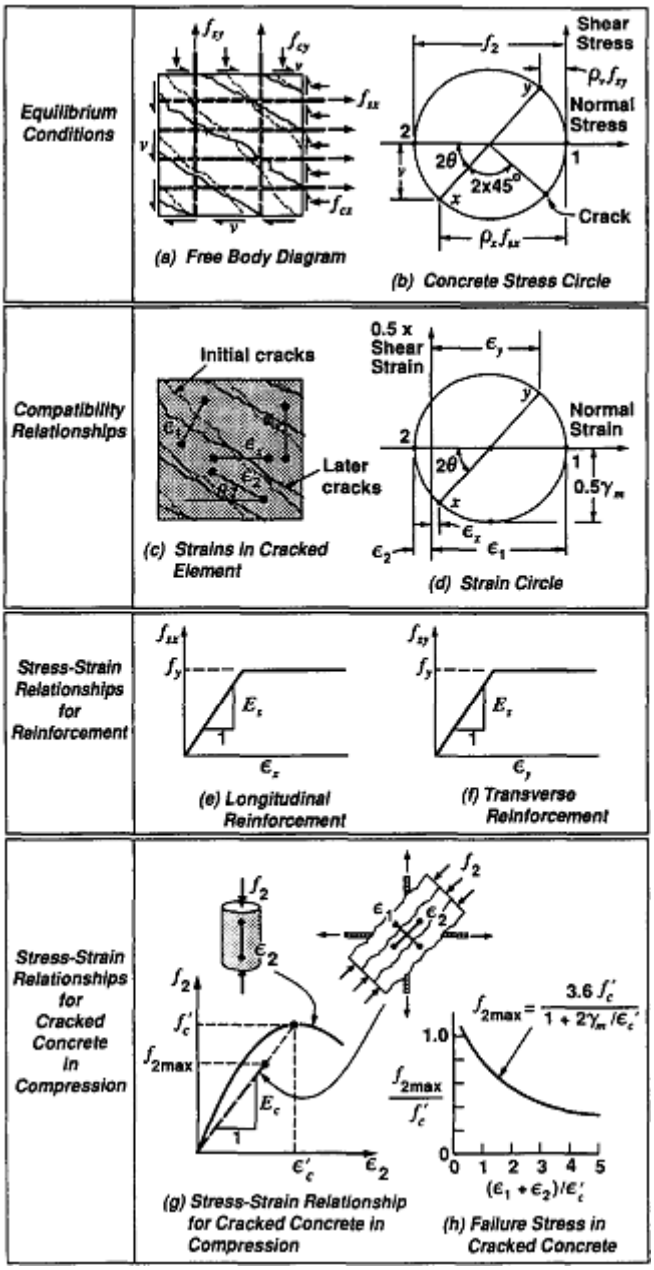


Figure 2-16 – Compression field theory (Mitchell and Collins 1974)

Before this equation can be used to determine θ, however, stress-strain relationships for the reinforcement and the concrete are required. It is assumed that the reinforcement strains are

related to the reinforcement stresses by the usual simple bilinear approximations shown in Figure 2-16(e and f). Thus, after the transverse strain, ε_y, exceeds the yield strain of the web reinforcements, the stress in the web reinforcements is assumed to equal the yield stress f_y, and **(16)** becomes identical to **(15)**.

Based on the results from a series of intensively instrumented beams, Collins (1978) suggested that the relationship between the principal compressive stress, f_2, and the principal compressive strain, ε_2, for diagonally cracked concrete would differ from the usual compressive stress-strain curve derived from a cylinder test[Figure 2-16(g)]. He postulated that as the strain circle becomes larger, the compressive stress required to fail the concrete, $f_{2,\max}$, becomes smaller [Figure 2-16(h)]. The relationships proposed were

$$f_{2\max} = \frac{3.6 f_c^{'}}{1 + 2\gamma_m / \varepsilon_c^{'}} \tag{20}$$

Where γ_m = diameter of the strain circle (that is, $\varepsilon_1 + \varepsilon_2$); and ε_c = strain at which the concrete in a cylinder test reaches the peak stress f_c'. For values of f_2 less than $f_{2,\max}$

$$\varepsilon_2 = \frac{f_2}{f_c^{'}\varepsilon_c^{'}} \tag{21}$$

It was suggested that the diagonally cracked concrete fails at a low compressive stress because this stress must be transmitted across relatively wide cracks. If the initial cracks shown in Figure 2-16(a) formed at 45^0 to the longitudinal reinforcement, and if θ is less than 45^0, which will be the case if ρ_v is less than ρ_x, then significant shear stresses must be transmitted across these initial cracks [Figure 2-16(b)]. The ability of the concrete to transmit shear across cracks depends on the width of the cracks, which, in turn, is related to the tensile straining of the concrete. The principal tensile strain, ε_1, can be derived from Figure 2-16(d) as

$$\varepsilon_1 = \varepsilon_x + (\varepsilon_x + \varepsilon_2)\cot^2\theta \tag{22}$$

For shear stresses less than that causing first yield of the reinforcement, a simple expression for the angle θ can be derived by rearranging the previous equations to give

$$\tan^4\theta = \left(1 + \frac{1}{n\rho_x}\right) \Big/ \left(1 + \frac{1}{n\rho_v}\right) \tag{23}$$

Where n = modular ratio E_s/E_c ; and E_c is taken as f_c'/ε_c . For the member shown in Figure 2-15, ρ_v is 0.0303, ρ_v is 0.00154, and n = 6.93; hence, **(23)** would give a θ value of 26.4^0. This would imply that the web reinforcements would yield at a shear stress of 1.62 MPa.

After the web reinforcements have yielded, the shear stress can still be increased if θ can be reduced. Reducing θ will increase the tensile stress in the longitudinal reinforcement and the compressive stress in the concrete. Failure will be predicted to occur either when the longitudinal steel yields, or when the concrete fails. For the member shown in Figure 2-15, failure of the concrete is predicted to occur when θ is lowered to 15.5^0, at which stage the shear stress is 2.89 MPa and ε_x is 1.73 x 10^{-3}. Note that these predicted values are for a section where the moment is zero. Moment will increase the longitudinal tensile strain ε_x, which will reduce the shear capacity. For example, if ε_x was increased to 2.5 x 10^{-3}, concrete failure would be predicted to occur when θ is 16.7^0 and the shear stress is 2.68 MPa.

2.3.2.3 Modified Compression Field Theory

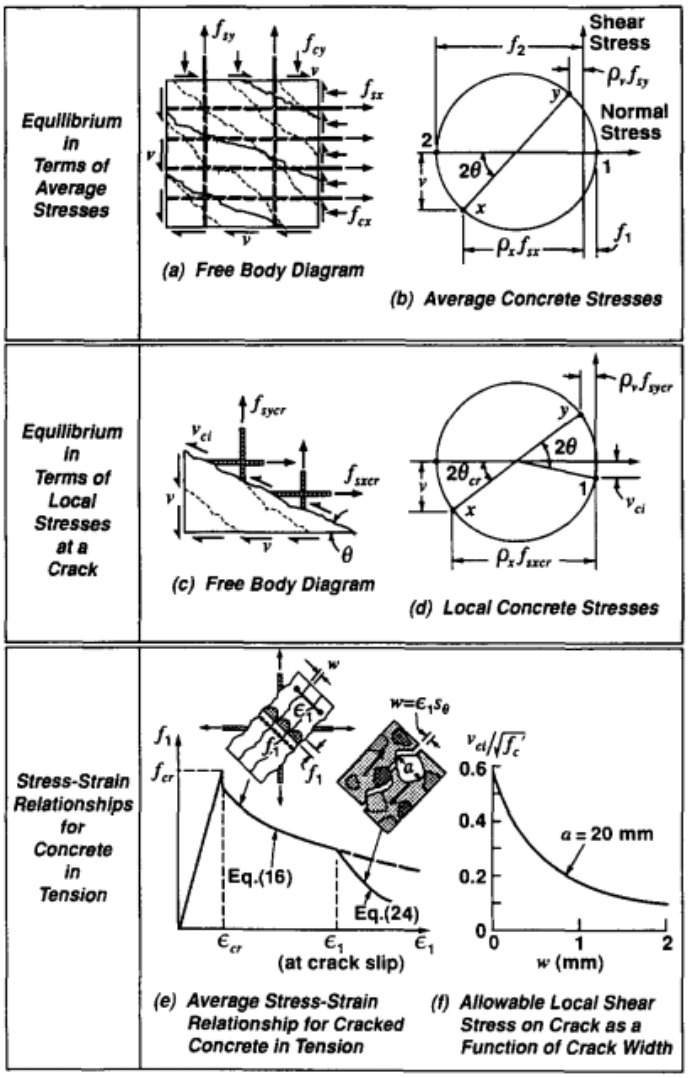


Figure 2-17 – Aspects of Modified Compression Field Theory

(ASCE-ACI Committee 445,1998)

The modified compression field theory (MCFT) (Vecchio and Collins 1986) is a further development of the CFT that accounts for the influence of the tensile stresses in the cracked concrete. It is recognized that the local stresses in both the concrete and the reinforcement vary from point to point in the cracked concrete, with high reinforcement stresses but low concrete tensile stresses occurring at crack locations. In establishing the angle θ from Wagner's equation, **(19)**, the compatibility conditions relating the strains in the cracked concrete to the strains in the reinforcement are expressed in terms of average strains, where the strains are measured over base lengths that are greater than the crack spacing [Figure 2-16(c and d)]. In similar manner, the equilibrium conditions, which relate the concrete

stresses and the reinforcement stresses to the applied loads, are expressed in terms of average stresses; that is, stresses averaged over a length greater than the crack spacing. These relationships can be derived from Figure 2-17(a and b) as

$$\rho_v f_{sy} = f_{cy} = \upsilon \tan\theta - f_1 \quad (24)$$

$$\rho_x f_{sx} = f_{cx} = \upsilon \cot\theta - f_1 \quad (25)$$

$$f_2 = \upsilon(\tan\theta + \cot\theta) - f_1 \quad (26)$$

These equilibrium equations, the compatibility relationships from Figure 2-16(d), the reinforcement stress-strain relationships from Figure 2-16(e and f), and the stress-strain relationships for the cracked concrete in compression enable the average stresses, the average strains, and the angle θ to be determined for any load level up to the failure.

Failure of the reinforced concrete element may be governed not by average stresses, but rather by local stresses that occur at a crack. In checking the conditions at a crack, the actual complex crack pattern is idealized as a series of parallel cracks, all occurring at angle θ to the longitudinal reinforcement and space a distance s_θ apart. From Figure 2-17(c and d), the reinforcement stresses at a crack can be determined as

$$\rho_v f_{sycr} = \upsilon \tan\theta - \upsilon_{ci} \tan\theta \quad (27)$$

$$\rho_x f_{sxcr} = \upsilon \cot\theta + \upsilon_{ci} \cot\theta \quad (28)$$

It can be seen that the shear stress, ν_{ci} , on the crack face reduces the stress in the transverse reinforcement but increases the stress in the longitudinal reinforcement. The maximum possible value of ν_{ci} is taken (Bhide and Collins 1989) to be related to the crack width, w, and the maximum aggregate size, a, by the relationship illustrated in Figure 2-17(f) and given by

$$\upsilon_{ci} \le \frac{0.18\sqrt{f_c'}}{\left(0.3 + \frac{24w}{a+16}\right)} \quad \text{(MPa, mm)} \quad (29)$$

The crack width, w, is taken as the crack spacing times the principal tensile strain, ε_1. At high loads, the average strain in the web reinforcements, ε_y, will typically exceed the yield strain of the reinforcement. In this situation, both f_{sy} in **(24)** and f_{sycr} in **(27)** will equal the yield stress in the web reinforcements. Equating the right hand sides of these two equations and substituting for ν_{ci} from **(29)** gives

$$f_1 \le \frac{0.18\sqrt{f_c'}\tan\theta}{\left(0.3+\frac{24w}{a+16}\right)} \tag{30}$$

Limiting the average principal tensile stress in the concrete in this manner accounts for the possibility of failure of the aggregate interlock mechanism, which are responsible for transmitting the interface shear stress, v_{ci} across the crack surfaces.

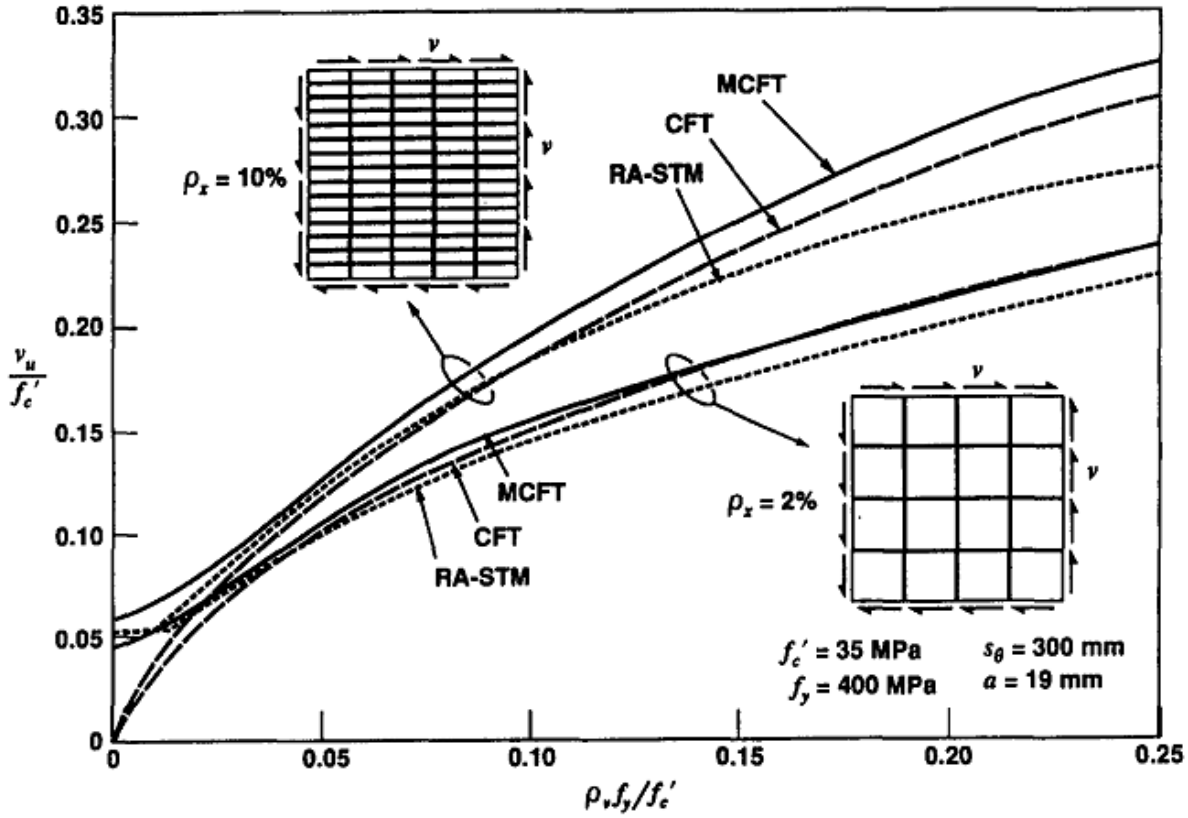


Figure 2-18 – Comparison of predicted shear strengths of two series of reinforced concrete elements (ASCE-ACI Committee 445,1998)

Figure 2-18 illustrates the influence of the tensile stresses in the cracked concrete on the predicted shear capacity of two series of reinforced concrete elements. In this figure, RA-STM stands for rotating –angle softened –truss model. If tensile stresses in the cracked concrete are ignored, as is done in the CFT, elements with no web reinforcements ($\rho_v = 0$) are predicted to have no shear strength.

2.4 Shear design procedures using Modified Compression Field theory

2.4.1 Design procedure based on Modified Compression Field Theory [5]

The relationships of the MCFT can be used to predict the shear strength of beams. Assuming that the shear stress in the web is equal to the shear force divided by the effective shear area, $b_w d_v$, and that, at failure, the web reinforcements will yield, equilibrium equations can be rearranged to give the following expression for the shear strength, V_n , of the section:

$$V_n = V_c + V_s + V_p \tag{31}$$

$$V_n = f_1 b_w d_v \cot\theta + \frac{A_v f_y}{s} d_v \cot\theta + V_p \tag{32}$$

$$V_n = \beta\sqrt{f'_c} b_w d_v + \frac{A_v f_y}{s} d_v \cot\theta + V_p \tag{33}$$

Where

V_c	Shear strength provided by tensile stresses in the cracked concrete
V_s	Shear strength provided by tensile stresses in the web reinforcements
V_p	Vertical component of the tension in inclined prestressing tendon
b_w	Effective web width, taken as the minimum web width within the shear depth
d_v	Effective shear depth, taken less than 0.9d
β	Concrete tensile stress factor indicating the ability of diagonally cracked concrete to resist shear

The shear stress that the web of a beam can resist is a function of the longitudinal straining in the web. The larger this longitudinal straining becomes, the smaller the shear stress required to fail the web. In determining the shear capacity of the beam, it is conservative to use the highest longitudinal strain, ε_x , occurring within the web. For design calculations, ε_x can be approximated as the strain in the tension chord of the equivalent truss. Hence

$$\varepsilon_x = \frac{\left(M_u/d_v\right) + 0.5N_u + 0.5V_u \cot\theta - A_{ps} f_{po}}{E_s A_s + E_p A_{ps}} \tag{34}$$

But need not be taken greater than 0.002,

Where

f_{po}	Stress in the tendon when the surrounding concrete is at zero stress, which may be taken as 1.1. times the effective stress in the prestressing, f_{se}, after all losses
A_s	Area of nonprestressed longitudinal reinforcement on the flexural tension side of the member
A_{ps}	Area of prestressed longitudinal reinforcement on the flexural tension side of the member
M_u	Moment at the section, taken as positive
N_u	Axial load at the section, taken as positive if tensile and negative if compressive

The determination of ε_x for a nonprestressed beam is illustrated in Figure 2-19 .

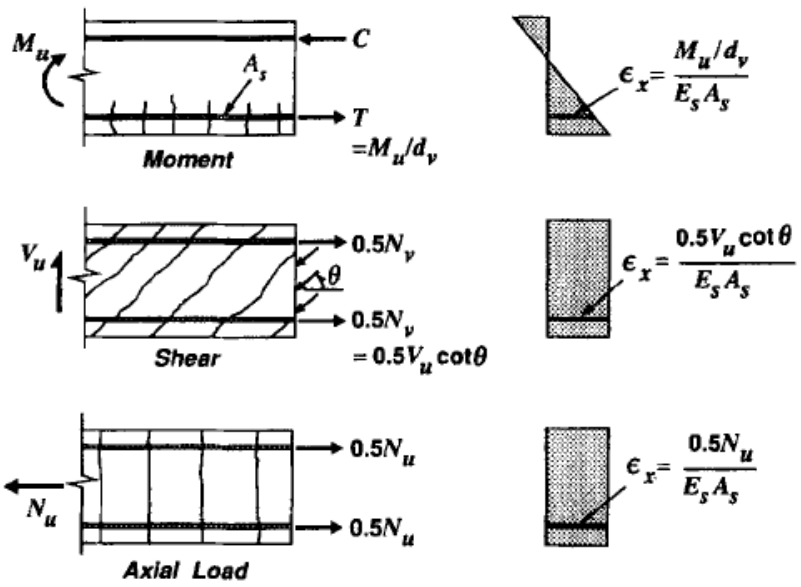


Figure 2-19 – Determination of strains, ε_x , for nonprestressed beam

(ASCE-ACI Committee 445,1998)

The longitudinal strain parameter, ε_x , accounts for the influence of moment, axial load, prestressing, and amount of longitudinal reinforcement on the shear strength of a section. If ε_x and the crack spacing s_θ are known, the shear capacity corresponding to a given quantity of web reinforcements can be calculated. This is equivalent to finding the values of β and θ.

Values of β and θ determined from the modified compression field theory and suitable for members with at least minimum web reinforcement are given in Figure 2-20

In determining these values it was assumed that the amount and spacing of the web reinforcements would limit the crack spacing to about 300 mm. the θ values given in figure ensure that the tensile strain in the web reinforcements, ε_v , is at least equal to 0.002 and that the compressive stress, f_2 , in the concrete does not exceed the crushing strength, $f_{2\max}$. Within the range of values of θ that satisfy these requirements, the values given in Figure 2-20 result in close to the smallest amount of total shear.

This design procedure has been the basis for the shear provision in AASHTO LRFD Bridge Design Specifications in 1994. However the graph for obtaining values of β and θ shown in Figure 2-20, were replaced by a table and simple rearrangement was done in some of the equations. [**9**] The overall iterative process of design in AASHTO LRFD can be summarized as follows.

1. Calculate shear stress demand v_u at a section and determine the shear ratio $\left(v_u/f_c'\right)$
2. Calculate ε_x at the section based on normal force (including p/s), shear and bending and an assumed value of θ
3. Longitudinal strain ε_x is the average strain at mid-depth of the cross section
4. Knowing $\left(v_u/f_c'\right)$ and ε_x, obtain the values of β and θ from the table
5. Recalculate ε_x based on revised value of θ; repeat iteration until convergence in θ is achieved.

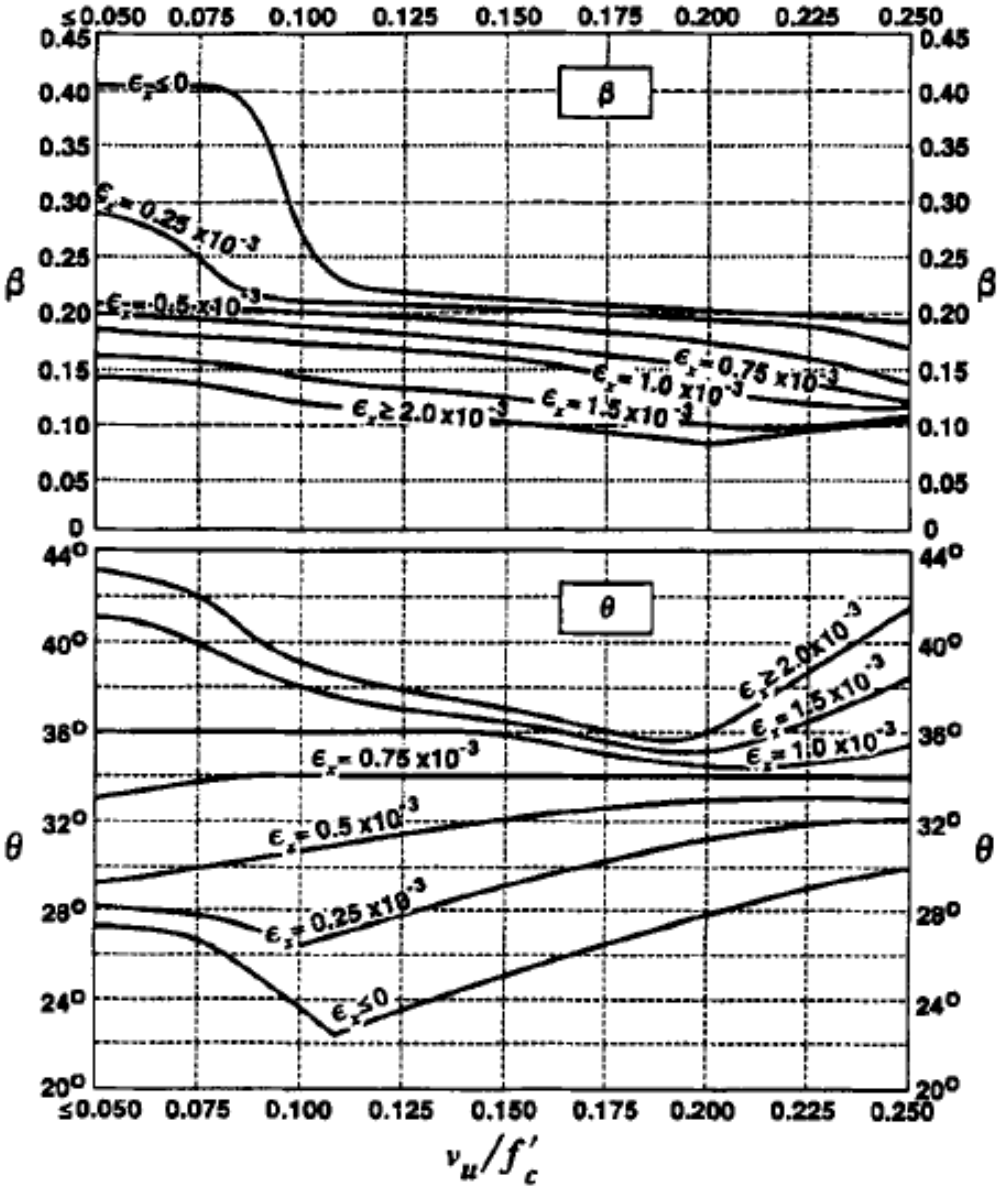


Figure 2-20 – Values of β and θ for members containing at least the minimum amount of web reinforcements (ASCE-ACI Committee 445,1998)

Table 2-1 – Values of β and θ for members with at least minimum shear reinforcement (AASHTO LRFD, 1994)

$\frac{v^*}{f'_c}$		Longitudinal Strain, $\varepsilon_x \times 1000$										
		≤ −0.20	≤ −0.10	≤ −0.05	≤ 0	≤ 0.125	≤ 0.25	≤ 0.50	≤ 0.75	≤ 1.00	≤ 1.50	≤ 2.00
≤ 0.075	θ	22.3°	20.4°	21.0°	21.8°	24.3°	26.6°	30.5°	33.7°	36.4°	40.8°	43.9°
	β	6.32	4.75	4.10	3.75	3.24	2.94	2.59	2.38	2.23	1.95	1.67
≤ 0.100	θ	18.1°	20.4°	21.4°	22.5°	24.9°	27.1°	30.8°	34.0°	36.7°	40.8°	43.1°
	β	3.79	3.38	3.24	3.14	2.91	2.75	2.50	2.32	2.18	1.93	1.69
≤ 0.125	θ	19.9°	21.9°	22.8°	23.7°	25.9°	27.9°	31.4°	34.4°	37.0°	41.0°	43.2°
	β	3.18	2.99	2.94	2.87	2.74	2.62	2.42	2.26	2.13	1.90	1.67
≤ 0.150	θ	21.6°	23.3°	24.2°	25.0°	26.9°	28.8°	32.1°	34.9°	37.3°	40.5°	42.8°
	β	2.88	2.79	2.78	2.72	2.60	2.52	2.36	2.21	2.08	1.82	1.61
≤ 0.175	θ	23.2°	24.7°	25.5°	26.2°	28.0°	29.7°	32.7°	35.2°	36.8°	39.7°	42.2°
	β	2.73	2.66	2.65	2.60	2.52	2.44	2.28	2.14	1.96	1.71	1.54
≤ 0.200	θ	24.7°	26.1°	26.7°	27.4°	29.0°	30.6°	32.8°	34.5°	36.1°	39.2°	41.7°
	β	2.63	2.59	2.52	2.51	2.43	2.37	2.14	1.94	1.79	1.61	1.47
≤ 0.225	θ	26.1°	27.3°	27.9°	28.5°	30.0°	30.8°	32.3°	34.0°	35.7°	38.8°	41.4°
	β	2.53	2.45	2.42	2.40	2.34	2.14	1.86	1.73	1.64	1.51	1.39
≤ 0.250	θ	27.5°	28.6°	29.1°	29.7°	30.6°	31.3°	32.8°	34.3°	35.8°	38.6°	41.2°
	β	2.39	2.39	2.33	2.33	2.12	1.93	1.70	1.58	1.50	1.38	1.29

*$v = V_u/b_v d_v$

Table 2-2 – Values of β and θ for members with less than minimum shear reinforcement (AASHTO LRFD, 1994)

s_{xe}* (in)		Longitudinal Strain, $\varepsilon_x \times 1000$										
		≤ −0.20	≤ −0.10	≤ −0.05	≤ 0	≤ 0.125	≤ 0.25	≤ 0.50	≤ 0.75	≤ 1.00	≤ 1.50	≤ 2.00
≤ 5	θ	25.4°	25.5°	25.9°	26.4°	27.7°	28.9°	30.9°	32.4°	33.7°	35.6°	37.2°
	β	6.36	6.06	5.56	5.15	4.41	3.90	3.26	2.86	2.58	2.21	1.96
≤ 10	θ	27.6°	27.6°	28.3°	29.3°	31.6°	33.5°	36.3°	38.4°	40.1°	42.7°	44.7°
	β	5.78	5.78	5.38	4.89	4.05	3.52	2.88	2.50	2.23	1.88	1.65
≤ 15	θ	29.5°	29.5°	29.7°	31.1°	34.1°	36.5°	39.9°	42.4°	44.4°	47.4°	49.7°
	β	5.34	5.34	5.27	4.73	3.82	3.27	2.64	2.27	2.01	1.68	1.46
≤ 20	θ	31.2°	31.2°	31.2°	32.3°	36.0°	38.8°	42.7°	45.5°	47.6°	50.9°	53.4°
	β	4.99	4.99	4.99	4.61	3.65	3.09	2.46	2.09	1.85	1.52	1.31
≤ 30	θ	34.1°	34.1°	34.1°	34.2°	38.9°	42.3°	46.9°	50.1°	52.6°	56.2°	59.0°
	β	4.46	4.46	4.46	4.43	3.39	2.82	2.19	1.84	1.61	1.30	1.10
≤ 40	θ	36.6°	36.6°	36.6°	36.6°	41.1°	45.0°	50.2°	53.7°	56.3°	60.2°	63.0°
	β	4.06	4.06	4.06	4.06	3.20	2.62	2.00	1.66	1.43	1.14	0.95
≤ 60	θ	40.8°	40.8°	40.8°	40.8°	44.5°	49.2°	55.1°	58.9°	61.8°	65.8°	68.6°
	β	3.50	3.50	3.50	3.50	2.92	2.32	1.72	1.40	1.18	0.92	0.75
≤ 80	θ	44.3°	44.3°	44.3°	44.3°	47.1°	52.3°	58.7°	62.8°	65.7°	69.7°	72.4°
	β	3.10	3.10	3.10	3.10	2.71	2.11	1.52	1.21	1.01	0.76	0.62

2.4.2 Design procedure based on the simplified Modified Compression Field Theory

Shear design procedures should be simple to understand and to use not only for ease of calculation but, more critically, for ease of comprehension. The engineer should be able to give physical significance to the parameters being calculated and to understand why they are important. If the procedures are simple enough, an experienced engineer should be able to perform at least preliminary calculations on the "back of an envelope." While the use of the required tables in the AASHTO LRFD shear design method is straightforward, it is not possible to remember the values on the table for "back of an envelope" calculations. Further, many engineers prefer simple equations to tables because they give a continuous range of values. To solve this problem and to make the shear design procedure of MCFT convenient for adopting in building codes, a simplified Modified Compression Field Theory was published in 2006. This theory used simple equilibrium and compatibility equations from the basic expressions of the MCFT to derive more convenient equations for the values of β and θ. [**2**]

The developed equations in the simplified MCFT are adopted in the shear provisions of AASHTO LRFD 2012 and Canadian code, CSA Committee 2004.

The nominal shear resistance is calculated as the sum of the concrete contribution and transverse reinforcement contribution, [**10**]

$$V_n = V_c + V_s + V_p \tag{35}$$

$$V_n = 0.25 f_c' b_v d_v + V_p \tag{36}$$

In which ;

$$V_c = 0.0316 \beta \sqrt{f_c'} b_v d_v \tag{37}$$

$$V_s = \frac{A_v f_y d_v \left(\cot\theta + \cot\alpha\right)\sin\alpha}{s} \tag{38}$$

For sections containing at least the minimum amount of transverse reinforcement, the value of β may be determined by

$$\beta = \frac{4.8}{\left(1 + 750\varepsilon_s\right)} \tag{39}$$

When sections do not contain at least the minimum amount of shear reinforcement, the value of β can be calculated as

$$\beta = \frac{4.8}{(1+750\varepsilon_s)}\frac{51}{(39+s_{xe})} \tag{40}$$

The value of θ in both cases may be as specified in

$$\theta = 29 + 3500\varepsilon_s \tag{41}$$

In equations (39) to (41), ε_s is the net longitudinal tensile strain in the section at the centroid of the tension reinforcement. In lieu of more involved procedures, ε_s may be determined by

$$\varepsilon_s = \frac{\left(\frac{|M_u|}{d_v} + 0.5N_u + |V_u - V_p| - A_{ps}f_{po}\right)}{E_sA_s + E_pA_{ps}} \tag{42}$$

The crack spacing parameter, s_{xe} , shall be determined as:

$$s_{xe} = s_x\frac{1.38}{a_g + 0.63} \tag{43}$$

Where:

A_c	Area of concrete on the flexural tension side of the member (in.^{2})
A_{ps}	Area of prestressing steel on the flexural tension side of the member (in.^{2})
A_s	Area of nonprestressed steel on the flexural tension side of the member at the section under consideration (in.^{2})
a_g	Maximum aggregate size (in.)
f_{po}	A parameter taken as modulus of elasticity of prestressing tendons multiplied by the locked in difference in strain between the prestressing tendons and the surrounding concrete
N_u	Factored axial force, taken as positive if tensile and negative if compressive (kip)
$\|M_u\|$	Absolute value of the factored moment, not to be taken less than $\|V_u - V_p\|d_v$ (kip-in.)
s_x	The lesser of either d_v or the maximum distance between layers of longitudinal crack control reinforcement, where the area of the reinforcement in each layer is not less than $0.003b_vs_x$ (in.)
V_u	Factored shear force (kip)

2.5 Building Codes and Shear Design Provisions

In a 1935 Engineering News Record Review article for structural design engineers, Professor Hardy Cross quoted with approval the paradoxical statement of the Cambridge astrophysicist Sir Arthur Eddington that "No experiment is worthy of credence unless supported by an adequate theory." For complex phenomena influenced by many variables understanding the meaning of particular experiments and the range of applicability of the results is extremely difficult unless the researcher is guided by an adequate theory which can identify the important parameters. [**11**]

Developing a comparable theory for the shear strength of reinforced concrete members has been the objective of a major worldwide research effort for more than 40 years. For members with significant amounts of shear reinforcement, a variable angle truss model based on the lower bound theory of plasticity has been developed and is incorporated into Eurocode 2. However for the potentially more dangerous cases of members without shear reinforcement, Eurocode 2 uses totally empirical procedures not "supported by an adequate theory". [**11**]

While flexural design is concerned with ensuring that the two sides of a member can resist the appropriate magnitudes of tensile or compressive longitudinal forces, shear design is intended to ensure that the two sides of the member continue to act as a unit. This involves identifying where shear reinforcement is required to link together the two sides of the member and determining how much of this reinforcement is needed to prevent a premature shear failure. For regions not containing shear reinforcement, a shear failure can occur without warning and typically involves the opening of a major diagonal crack. Traditional American shear design procedures assumed that such failures of members without shear reinforcement would not occur if the calculated shear stress, $V/(b_w jd)$, at service loads was less than about $0.03f_c'$. If the shear stress was higher than this allowable stress, than shear reinforcement (e,g, links) would be added to carry the excess. The capacity added by the links was given by the 45^0 truss model of Ritter and Morsch as $\rho_w f_s$ where f_s was the allowable tensile stress in the links. Such shear reinforcement controls the opening of diagonal cracks and permits much higher shear stresses to be resisted. Irrespective of the amount of links, however, an upper limit of $0.12f_c'$ was placed on the shear stress at service load. In traditional German shear design, by contrast, once the shear stress at service load exceeded about 0.4 MPa, shear reinforcement was provided to carry the entire shear using the 45^0 truss

model. Because of these differences in shear design requirements, American reinforced concrete beams typically contained much less shear reinforcement than comparable German beams. [**11**]

2.5.1 Overview of current ACI Design Procedures (ACI 318-14)

The current ACI design procedure for shear defines the nominal shear strength as the sum of the shear strength provided by shear reinforcement, V_S , and the shear strength provided by concrete, V_c , which is assumed to be the same for beams with and without shear reinforcement and is taken as the shear causing significant inclined cracking.

The value of V_c is defined for members subject to shear and flexure only and for members subject to axial compression separately. Two alternatives are presented for calculation of V_c . The first alternative has a simple formula. Unlike its European counterpart, the ACI provision for calculation of the concrete contribution doesn't contain the longitudinal reinforcement ratio as a factor. It only depends on the compressive strength of the concrete and the size of the member.

The second alternative contains a more detailed calculation. In this case, many factors including ρ_w and $V_u d / M_u$ are shown to affect the concrete contribution.

The contribution of the shear reinforcement is based on the modified truss analogy. As it is presented in the commentary, the truss analogy assumes that the total shear is carried by shear reinforcement. However, considerable research has indicated that shear reinforcement needs to be designed to carry only the shear exceeding that which causes inclined cracking, provided the diagonal members in the truss are assumed to be inclined at 45 degrees. Thus, the ACI approach of calculating the shear reinforcement contribution can be generalized as modified 45 degree truss analogy.

Shear reinforcement restrains the growth of inclined cracking. Ductility is increased and a warning of failure is provided. In an unreinforced web, the sudden formation of inclined cracking might lead directly to failure without warning. Such reinforcement is of great value if a member is subjected to an unexpected tensile force or an overload. Accordingly, due to the reason stated above, a provision for providing minimum shear reinforcement for all members except for solid slabs, footings and joists is stipulated in ACI318.

2.5.2 Overview of Recent European Codes (EN 1992:2004)

In the current European Code, the shear resistance of a member with shear reinforcement is defined to be the shear resistance offered by the web reinforcements. Shear reinforcement is not necessary if the resulted shear force is less than the member design shear resistance without shear reinforcement. However minimum shear reinforcement is required except in slabs and members of minor importance.

An empirical formula is given for calculation of the contribution from the concrete in resisting shear. The empirical formula for concrete contribution takes into account the longitudinal reinforcement ratio, the compressive stress capacity of the concrete and the presence of axial force.

The calculation of shear force resistance contribution of the transverse reinforcement is based on the variable angle Truss analogy. Unlike the ACI, this code doesn't have a specific value for the crack inclination angle θ. But it gives a recommended limit of $1 < \cot\theta < 2.5$. On the other hand, following the Truss analogy, it gives a maximum limit for the shear force to insure that the diagonal compression force will not exceed the diagonal crushing force of the concrete, νf_{cd} where ν is 0.6 for concrete grades greater than 60 MPa and $0.9 - f_{ck} / 200 > 0.5$ for concrete grades greater than 60 MPa.

As per the variable angle truss analogy (section 2.3.1.1), there is an additional tensile stress that will be resulted on the longitudinal reinforcement and European code has a provision to take care of this additional tensile stress as per the analogy.

CHAPTER 3 BUILDING CODES AND EFFECT OF SPACING

This chapter is dedicated for the revision of different building codes and the relationship between their provision of shear capacity calculation and spacing of web reinforcement. As shown in the table below, 12 selected widely used building codes are reviewed and a summary is enumerated below.

1. Except the AASHTO LRFD (2002) and CSA, all of the codes provision of shear capacity contribution from the web reinforcement is based on the truss analogy.
2. The CSA (1994) and AASHTO LRFD (2002) are based on the basic modified compression field theory but the use of tables to calculate the necessary factors made them inconvenient for designers because the provisions require a trial and error rigorous procedure.
3. The CSA (2004) and AASHTO LRFD (2012) are based on the simplified compression field theory which made the calculation of the crack angle straight forward.
4. Except for the codes that applied the MCFT for their provisions, all of the codes founded their provisions of the concrete contribution from empirical equations.
5. All of the reviewed codes do not consider spacing of web reinforcement as a factor affecting the capacity[2].
6. In ACI 318-02, AASHTO standard and ASBI, the calculated value for V_c is an estimate of the diagonal cracking load. This approach was considered useful for both assessing the condition of a member in the field and for checking whether or not the member was expected to be cracked in shear under service loads.
7. The AASHTO LRFD specifications require a larger minimum amount of shear reinforcement than most other codes.
8. The CSA A23.3-04, AASHTO (1979), AASHTO LRFD, Eurocode 2, JSCE, and DIN all enable the designer to use an angle of diagonal compression flatter than 45 degrees when evaluating the contribution of shear reinforcement to shear capacity.

[2] There is a spacing parameter "s" in all of the provisions but this parameter is normalized to be ratio of web reinforcement because it is expressed as A_v/s. This means providing a reinforcement of area "A" at a spacing "s" yields the same capacity as providing an reinforcement of area "2A" at a spacing "2s".

Table 3-1 – Comparison of different design approaches (units: psi ,in ,lbs)

Approaches	V_c	V_s	$V_{n,\max}$	$A_{v,\min}$
ACI318-02	$V_c = 2\sqrt{f'_c}\,b_w d$ (empirical eq.)	$V_s = \dfrac{A_v f_y d}{s}$	$V_c + 8\sqrt{f'_c}\,b_w d$	$0.75\sqrt{f'_c}\dfrac{b_w s}{f_y} \geq \dfrac{50 b_w s}{f_y}$
ACI 318-14	$V_c = 2\lambda\sqrt{f'_c}\,b_w d$ (empirical eq.)	$V_s = \dfrac{A_v f_y d}{s}$	$V_c + 8\sqrt{f'_c}\,b_w d$	$0.75\sqrt{f'_c}\dfrac{b_w s}{f_y} \geq \dfrac{50 b_w s}{f_y}$
AASHTO STD (1989)	$V_c = 2\sqrt{f'_c}\,b_w d$ (empirical eq.)	$V_s = \dfrac{A_v f_y d}{s}$	$V_c + 8\sqrt{f'_c}\,b_w d$	$\dfrac{50 b_w s}{f_y}$
CSA (1994)	$V_c = \beta\sqrt{f'_c}\,b_v d_v$ (derived from MCFT) β is given in Table as a function of ε_x , (v/f'_c or s_{xe})	$V_s = \dfrac{A_v f_y d\cot\theta}{s}$ θ is given in Table as a function of ε_x , (v/f'_c or s_{xe})	$0.25 f'_c b_v d_v + V_p$	$0.72\sqrt{f'_c}\dfrac{b_w s}{f_y}$
AASHTO LRFD (2002)	$V_c = \beta\sqrt{f'_c}\,b_v d_v$ (derived from MCFT) β is given in Table as a function of ε_x , (v/f'_c or s_{xe})	$V_s = \dfrac{A_v f_y d\cot\theta}{s}$ θ is given in Table as a function of ε_x , (v/f'_c or s_{xe})	$0.25 f'_c b_v d_v + V_p$	$\sqrt{f'_c}\dfrac{b_v s}{f_y}$

Approaches	V_c	V_s	$V_{n,\max}$	$A_{v,\min}$
CSA (2004)	$V_c = \beta\sqrt{f'_c}\,b_v d_v$ (derived from MCFT) $\beta = \frac{4.8}{(1+1500\varepsilon_x)}\frac{51}{(39+s_{xe})}$ $\varepsilon_x = \frac{M_n/d_v + 0.5N_u + V_u - \phi_p V_p - A_{po}f_{po}}{2(E_s A_s + E_p A_{po})}$	$V_s = \frac{A_v f_y d\cot\theta}{s}$ $\theta = 29 + 7000\varepsilon_x$	$0.25 f'_c b_v d_v + V_p$	$0.72\sqrt{f'_c}\frac{b_w s}{f_y}$
EC2 (1991)	– Standard method: $V_c = 0.2758 k\beta(f_{ck})^{2/3}(1.2+40\rho_t)b_w d$ (empirical eq.) Where $1.0 \le \beta = \frac{2.5d}{x} \le 5.0$ $k = 1.6 - 0.0254d \ge 1.0$ – Variable- angle truss method: $V_c = 0$	– Standard method: $V_s = \frac{A_v f_y d(0.9d)}{s}$ – Variable-angle truss method: $V_s = \frac{A_v f_y d(0.9d)\cot\theta}{s}$ Where $0.4 < \cot\theta < 2.5$ but for beams with curtailed longitudinal reinforcement: $0.5 < \cot\theta < 2.0$	– Standard method: $0.5\nu(0.67 f_{ck})b_w(0.9d)$ $\nu = 0.7 - \frac{f_{ck}}{29000} \ge 0.5$ – Variable-angle truss method: $\frac{\nu(f_{ck}/1.5)b_w(0.9d)}{\cot\theta + \tan\theta}$ Where cotθ can be obtained as: $\cot\theta \le \sqrt{\left(\frac{\nu(f_{ck}/1.5)}{\rho_v f_y} - 1\right)}$	For $f'_c \le 2800\ psi$: $\rho_v f_y \ge 0.35$ For $f'_c \le 4800\ psi$: $\rho_v f_y \ge 0.52$ For $f'_c \le 6900\ psi$: $\rho_v f_y \ge 0.64$
AASHTO LRFD (2012)	$V_c = 0.0316\beta\sqrt{f'_c}\,b_v d_v$ (derived from MCFT) $\beta = \frac{4.8}{(1+1500\varepsilon_x)}\frac{51}{(39+s_{xe})}$ $\varepsilon_x = \frac{M_n/d_v + 0.5N_u + V_u - V_p - A_{po}f_{po}}{E_s A_s + E_p A_{po}}$	$V_s = \frac{A_v f_y d\cot\theta}{s}$ $\theta = 29 + 3500\varepsilon_x$	$0.25 f'_c b_v d_v + V_p$	$0.0316\sqrt{f'_c}\frac{b_v s}{f_y}$

Approaches	V_c	V_s	$V_{n,\max}$	$A_{v,\min}$
EC2 (2003)	– For members without shear reinforcement: $V_c = \left[3.31k\left(100\rho_t f_{ck}\right)^{1/3} - 0.15N_u/A_c\right]b_w d$ $\geq \left(\nu_{\min} - 0.15N_u/A_c\right)b_w d$ (empirical eq.) Where $\nu_{\min} = 0.4215k^{3/2}f_{ck}{}^{1/2}$ $k = 1 + \sqrt{\frac{7.87}{d}} \leq 2.0$ – For members with shear reinforcement: $V_c = 0$	$V_s = \frac{A_v f_y d\left(0.9d\right)\cot\theta}{s}$ Where $1 \leq \cot\theta \leq 2.5$	$\left[\alpha_{cw}\nu_1 \frac{\left(0.67f_{ck}\right)}{\cot\theta + \tan\theta}\right]b_w z$ α_{cw} taking account of axial compressive stress, $\nu_1 = 0.6\left(1 - f_{ck}/36250\right)$ Cotθ can be obtained as: $\cot\theta \leq \sqrt{\left(\frac{\alpha_{cw}\nu_1\left(f_{ck}/1.5\right)}{\rho_v f_y} - 1\right)}$	$\frac{0.00664\sqrt{f_{ck}}}{f_y}$
DIN (2001)	– For members without shear reinforcement: $V_c = \left[2.76k\left(100\rho_t f_{ck}\right)^{1/3} - 0.12N_u/A_c\right]b_w d$ Where $k = 1 + \sqrt{\frac{7.87}{d}} \leq 2.0$ (empirical eq.) – For members with shear reinforcement: $V_c = \left[6.63f_{ck}{}^{1/3}\left(1 - 1.2\frac{N_u/A_c}{\left(0.67f_{ck}\right)}\right)\right]b_w\left(0.9d\right)$ (empirical eq.)	$V_s = \frac{A_v f_y d\left(0.9d\right)\cot\theta}{s}$ Where $\cot\theta = \frac{\left(1.2 - 1.4\frac{N}{A_C}/\left(0.57f_{ck}\right)\right)}{\left(1 - V_c/V_u\right)}$ But $0.58 \leq \cot\theta \leq 3.0$	$\frac{\left(0.67f_{ck}\right)}{\cot\theta + \tan\theta}b_w\left(0.9d\right)$	$\frac{0.0025\left(f_{ck}\right)^{2/3}}{f_y}$
JSCE (1986)	$V_c = 0.9\beta_d\beta_p\beta_n\left(f_c'\right)^{1/3}b_w d$ (empirical eq.) $\beta_d = \left(39.4/d\right)^{1/4} \leq 1.5$ $\beta_d = \left(100\rho_w\right)^{1/3} \leq 1.5$ $0 \leq \beta_n \leq 2.0$:taking account of moment and axial compressive stress	$V_s = \frac{A_v f_y d\left(0.87d\right)}{s}$	$15\sqrt{f_c'}b_w d$	$0.0015b_w s$

Approaches	V_c	V_s	$V_{n,\max}$	$A_{v,\min}$
JSCE (2002)	$V_c = 0.9\beta_d\beta_p\beta_n\left(f'_c\right)^{1/3} b_w d$ (empirical eq.) $\beta_d = \left(39.4/d\right)^{1/4} \le 1.5$ $\beta_d = \left(100\rho_w\right)^{1/3} \le 1.5$ $0 \le \beta_n \le 2.0$:taking account of moment and axial compressive stress	$V_s = \dfrac{A_v f_y d\left(0.87d\right)}{s}$	$15\sqrt{f'_c} b_w d$	$0.0015 b_w s$

Note: When there is more than one approach in a shear design provision, the most commonly used one is summarized in this table

Evaluation of shear design methods by NCHRP using test Database [**9**]

To evaluate the accuracy of different national codes of practice, a large experimental database was used to evaluate the shear strength ratio $\left(V_{test}/V_{code}\right)$ for six different Codes for 1,359 selected beam tests results. Following a brief description of the experimental database, the results of this evaluation are summarized.

The 1,359 – member database consists of 878 reinforced concrete (RC) and 481 prestressed concrete (PC) members. These members were selected from the larger shear database so that members in which significant arch action or flexural failures were suspected were removed from the database. Most of the RC members had rectangular cross sections and were simply supported using bearings positioned underneath the member. Of these, 718 did not contain shear reinforcement and 160 did. The PC members consisted of rectangular, T-shaped, and I-shaped sections and most of the members were simply supported, again on bearings positioned under-neath the member. Of these, 321 did not contain shear reinforcement and 160 did. About 80 percent of both the members in the RC and PC components of the database had depths less than 20 inches.

Table 4 presents an examination of the Shear Strength Ratios $\left(V_{test}/V_{code}\right)$ and Coefficients of Variation (COV) for ACI 318-02, AASHTO LRFD Bridge Design Specifications (2001), CSA A23.3-04, JSCE Code (1986), Eurocode (EC2 2003), and the German Code (DIN, 2001). The code calculated strengths are nominal capacities and therefore all resistance and strength reduction factors are set to 1.0. As a result, the calculated strengths by ACI 318-02 would be equivalent to the calculated strengths by the AASHTO Standard Specifications (16^{th} edition). In this table, the mean and COV are presented for seven segment of the database, all members, all RC members, all RC members without shear reinforcement, all RC members with shear reinforcement, all PC members without shear reinforcement, and all PC members with shear reinforcement.

Table 3-2 – Code assessment for RC and PC members

Member Type		All	RC	RC	RC	PC	PC	PC
With or Without Av			Both	No Av	With Av	Both	No Av	With Av
Count	(#)	1359	878	718	160	481	321	160
ACI	Mean	1.44	1.51	1.54	1.35	1.32	1.38	1.21
	COV	0.371	0.404	0.418	0.277	0.248	0.247	0.221
LRFD	Mean	1.38	1.37	1.39	1.27	1.40	1.44	1.32
	COV	0.262	0.262	0.266	0.224	0.261	0.290	0.154
CSA	Mean	1.31	1.25	1.27	1.19	1.41	1.46	1.31
	COV	0.275	0.274	0.282	0.218	0.261	0.287	0.147
JSCE	Mean	1.51	1.36	1.35	1.38	1.80	1.85	1.70
	COV	0.321	0.280	0.293	0.216	0.292	0.297	0.272
EC2	Mean	1.85	1.74	1.75	1.70	2.06	2.13	1.91
	COV	0.409	0.336	0.328	0.373	0.470	0.343	0.687
DIN	Mean	2.05	1.95	2.10	1.25	2.25	2.59	1.58
	COV	0.395	0.368	0.327	0.267	0.413	0.345	0.357

COV – Coefficient of variation

From

Table 3-2, the following observations can be made:

- The AASHTO LRFD and CSA approaches were best able to predict the capacity of the members in this data-base. The mean of the strength ratios for both of these approaches was very consistent across the different categories of selected members and of a value (1.19 – 1.46) that would be expected to result in conservative designs that made reasonably efficient use of shear reinforcement. The small COV was particularly impressive for PC members with shear reinforcement.
- The close correlation between the means and COV for the AASHTO LRFD and CSA methods indicates that these two methods would yield similar designs in terms of the amount of required shear reinforcement. As a result, it is concluded that the equations for calculating β , θ , and ε_x in CSA A23.3-04 are reasonable replacements for the tables and the old equation for ε_x of AASHTO LRFD that could result in an iterative design approach.
- Although the overall COV for the ACI (AASHTO Standard Specifications) approach is about 40 percent greater than the least overall COV, this results principally from the

poor performance of these design provisions in predicting the capacity of RC members that do not contain shear reinforcement. Both the mean and COV of the ACI (AASHTO Standard Specifications) method for RC and PC members with shear reinforcement were quite good. Regarding the prediction of RC members without shear reinforcement, given the measured shear capacity of many of the members, the ACI (AASHTO Standard Specifications) approaches would frequently have required designs with minimum shear reinforcement because of the rule that $A_{v,\min}$ is required when $V_u \geq \phi V_c / 2$.

- The JSCE code was somewhat better than the ACI (AASHTO Standard Specifications) approach at calculating the shear strength of RC members, but very conservative at calculating the shear strength of prestressed concrete members. This conservatism results from a limitation in the Japanese code of only doubling V_c due to the effect of prestressing and because a 45-degree parallel chord truss model is used in calculating the contribution of the shear reinforcement.
- Both the EC2 and DIN Codes were considerably less successful in predicting the capacity of members in the shear database. There was a surprising large variation in the means across the different categories of members.

CHAPTER 4 EXPERIMENTAL PROGRAM

This chapter describes the experimental program completed at the Construction Materials Laboratory, Addis Ababa Institute of Technology to study the effect of spacing and configuration of web reinforcement on the shear behavior of reinforced concrete beams.

The main variable used in the current study is spacing and configuration of web reinforcement. A 2.2 m long beam was selected for the experimental program and shear failure was ensured by providing high strength longitudinal reinforcement bar. Prior to the experiment, shear failure was further confirmed by comparing the flexural and shear capacity using hand calculation and by modeling the beam on Response2000.

Three specimens were selected. All the three specimens had similar cross section, longitudinal reinforcement, and web reinforcement ratio. Thus the shear capacity of all the three specimens according to widely accepted codes including the Eurocode and ACI is the same.

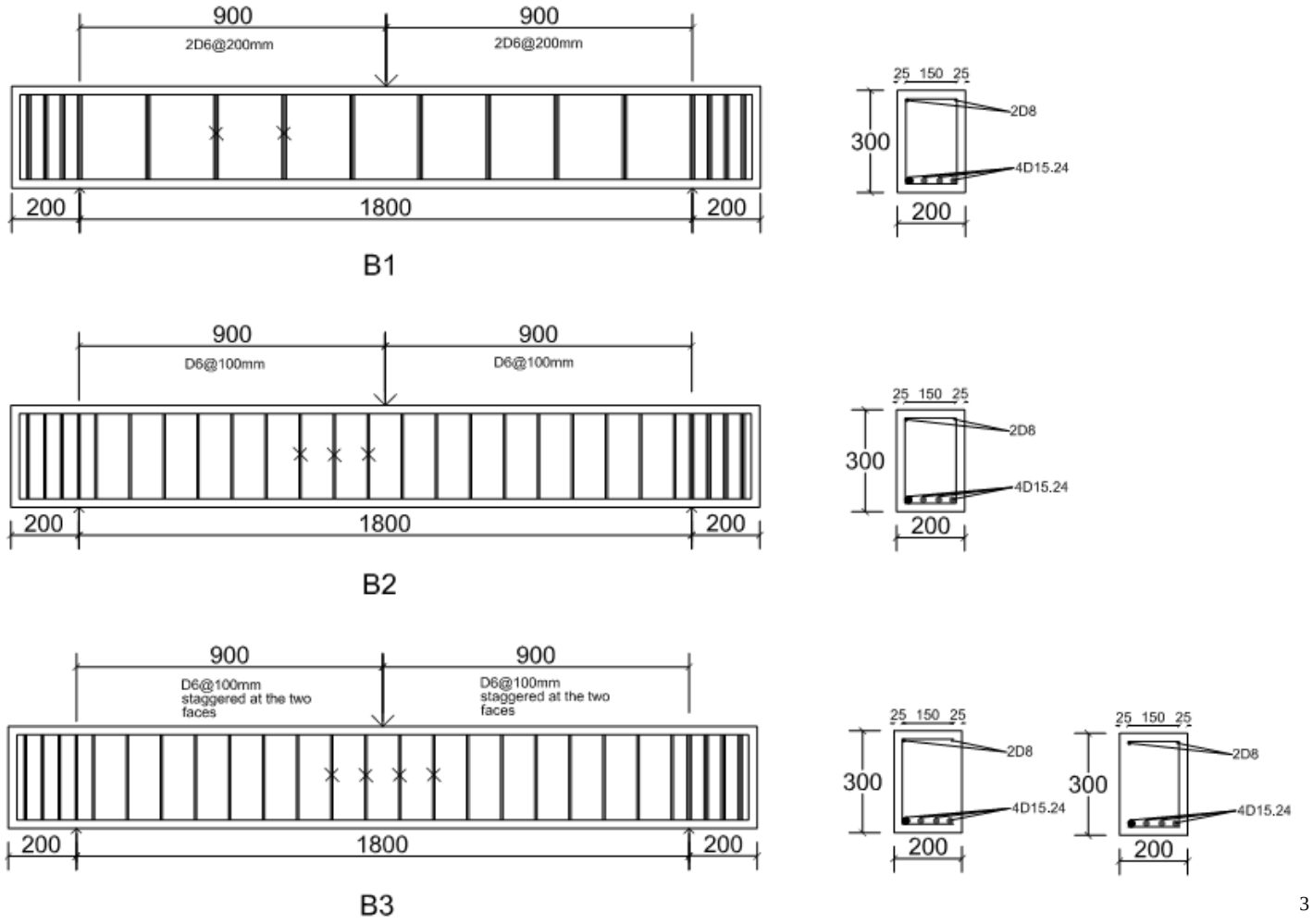
4.1 Specimens

The experimental program consists of 3 simply supported RC beam specimens with rectangular cross section and constant breadth (b) and Depth (D) of 200 mm and 300 mm respectively. Figure 4-1 shows details and reinforcement arrangement of the specimens.

The shear reinforcement in Specimens B1 and B2 is closed web reinforcement. The shear reinforcement in Specimen B3 doesn’t have symmetrical arrangement on the longitudinal direction. One of the shear spans contains single leg web reinforcements staggered at the two faces of the beam and the other shear span contains closed leg web reinforcements inclined on its horizontal face to have a staggered arrangement.

Table 4-1 – Details of investigated specimens

Specimen	**Overall height h, (mm)**	**Effective depth d, (mm)**	**Shear span a, (m)**	**a/d**	**Side concrete cover to web reinforcement ,(mm)**	ρ_t **%**	ρ_w **%**	**Web reinforcement spacing (mm)**
B1	300	262	0.9	3.435	25	0.6		200
B2	300	262	0.9	3.435	25	0.6		100
B3	300	262	0.9	3.435	25	0.6		200 (Staggered)



[3]

Figure 4-1 – Experiment specimens

[3] X : shows locations of strain gauges

4.2 Materials

4.2.1 Concrete

All the three specimens were cast in metal molds using cast in situ concrete. During the casting process of concrete, samples of concrete cylinders were prepared in a cylinder of diameter 100mm and height 200 mm. 6 cylinders were taken from each beam specimen and 3 of them were tested 14 days after the casting day and the rest 3 samples were tested 21 days after the casting day (Table 4-3). In the mix proportions of concrete, ordinary Portland cement was used and water-cement ratio was kept at 0.55. (See Table 4-4)

Cylinders were tested using a compression testing machine (shown in Figure 4-2). The maximum load achieved was used to calculate the ultimate stress of each cylinder.



Figure 4-2 - Compressive strength testing machine

Table 4-2 – 14th day strength of cylinder samples

Specimen	Compressive strength (MPa)			
	Cylinder 1	**Cylinder 2**	**Cylinder 3**	**Average**
B1	15.05	14.74	11.66	13.82
B2	13.08	14.60	16.98	14.89
B3	12.24	18.95	7.24	12.81

Table 4-3 – 21st day strength of cylinder samples

Specimen	Compressive strength (MPa)			
	Cylinder 1	**Cylinder 2**	**Cylinder 3**	**Average**
B1	16.01	12.22	12.30	13.51
B2	14.24	13.95	17.56	15.25
B3	18.02	10.92	13.73	14.22

Table 4-4 – Mix proportions of concrete

Average cylindrical strength	14.33 MPa
Cement type	Ordinary Portland cement
Maximum aggregate size	25 mm
Free-water content	180 kg/m^3
Cement content	330 kg/m^3
Coarse aggregate content	1075 kg/m^3
Fine aggregate content	795 kg/m^3
Water-cement ratio	0.55

4.2.2 Steel

In all test specimens, plain reinforcement bar with a diameter of 6 mm was used for the shear reinforcement and high strength tendons were used for the bottom reinforcement. Tension

tests were conducted on the web reinforcement steel to determine the stress-strain characteristics. The longitudinal bars were high strength tendons and tension tests were not conducted due to their complex property. Rather, the property of these tendons was obtained from the manufacturer's manual. The mechanical properties of reinforcements used are given in Table 4-5.



Figure 4-3 - Tensile Strength testing machine

Table 4-5 – Mechanical properties of reinforcement

Bar diameter (mm)	**Area (mm^2)**	**Yield strength (MPa)**	**Elastic modulus X 10^3 (MPa)**	**Ultimate strength (MPa)**
D 15.24	141.4	1847	201012	1992
D 6	28.27	251.11	2000000	321.85

4.3 Specimen Fabrication

This section describes in brief the details of the specimen construction process. The test specimens were constructed at the Construction Materials Laboratory. First, the reinforcement cages were assembled outside the forms. During the fabrication of the cages, the web reinforcement spacing was carefully controlled to follow the design. Figure 4-5 shows the steel cage after assembly.



Figure 4-4 - Reinforcement cage of specimen B2

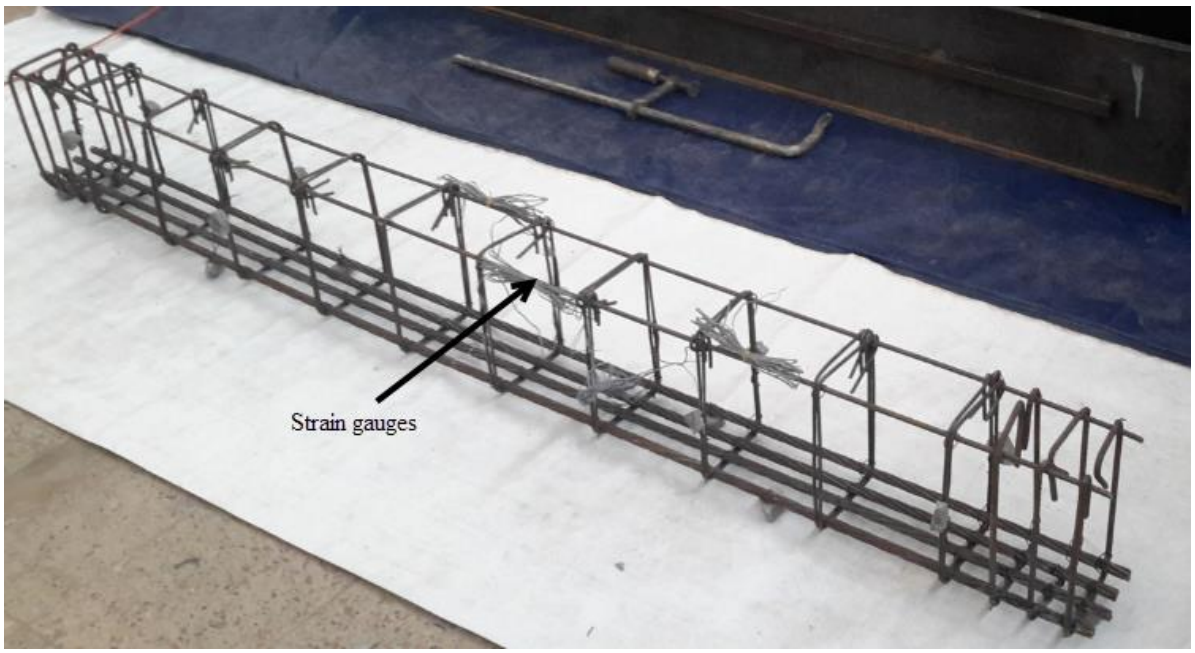


Figure 4-5 - Reinforcement cage of Specimen B1

Metal sheet forms were constructed in the Mechanical Engineering Laboratory of AAiT. The formworks were griped at the mid span to avoid bulging of concrete during casting. After the formwork was erected, form release agent was applied on the inner surface of the forms for easy stripping of formwork. Once the formwork was ready, the steel cages were placed inside, maintaining a concrete clear cover of 25 mm on all sides as shown in Figure 4-6



Figure 4-6 - Reinforcement cage of specimen B1 inside the formwork

Concrete was casted in the laboratory and an electric vibrator was used to consolidate the concrete. The concrete surface exposed to air was moist cured by covering the beams with wet cotton and by casing it with a plastic sheet to avoid evaporation.

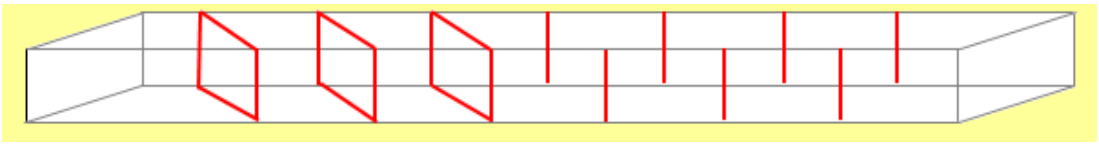


Figure 4-7 – 3D sketch for web reinforcement configuration in specimen B3

4.4 Test Setup

The beam was setup on steel plates with a roller in between the plates. The steel roller supports were installed on concrete members anchored to the strong floor. A concentrated load was applied using a hydraulic jack (shown in Figure 4-8) of maximum capacity 300 kN. Figure 4-9 shows the test setup.



Figure 4-8 – Hydraulic Jack



Figure 4-9 - Test Setup

4.5 Instrumentation

All beams were fully instrumented to measure the applied loads on the beams, the deflections and strain in transverse steel. In brief, the instrumentation consisted of a load cell which measures the applied load (shown in Figure 4-11), deflection measurement tool (shown in Figure 4-10) for the mid span deflection and strain gauges assembled on some of the web reinforcements. All of the instrumentations were connected to a data logger and the experimental data was directly obtained in a USB stick (shown in Figure 4-12).



Figure 4-10 - Displacement measuring tool



Figure 4-11 - Load Cell



Figure 4-12 - Data Logger

CHAPTER 5 FEM ANALYSIS USING DUCOM-COM3

5.1 About the software

For the analytical simulation of this study, the DuCOM-COM3 system which is developed in the University of Tokyo is used. This is a multi-scale analysis code that links the thermo-chemo-physics platforms DuCOM and COM3. DuCOM is an integrated thermo-hygro analysis code that includes cement hydration in concrete mixture, micro-pore structure formation and mass transport models for concrete ranging from 10^{-3} to 10^{-9} meter scales of micro-voids, while COM3 is a 3D finite-element analysis platform for structural concrete with and without cracks. As a result, DuCOM-COM3 is capable of predicting the change in concrete material properties from casting to dismantling of entire structures and taking this material development into account for predicting the response of structural concrete. With this integration, the long-term structural response under actual ambient conditions can be predicted in a realistic manner.

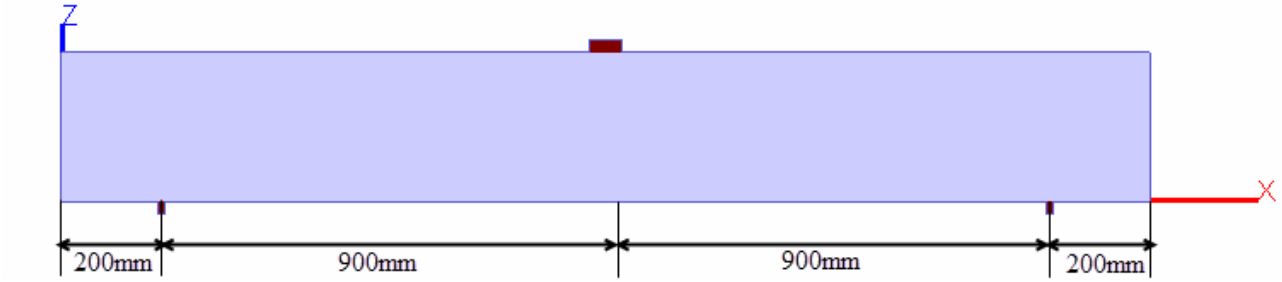
5.2 Specimens

Three - dimensional nonlinear finite element analyses were carried out for 15 specimens. The specimens were categorized in three series to study the effect of concrete grade in relation to spacing and arrangement of web reinforcement. Table 5-1 shows the cross sectional property and reinforcement detailing of the 15 specimens.

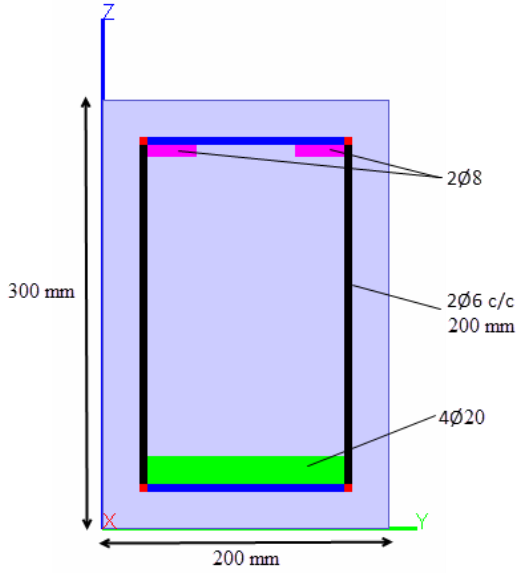
Table 5-1 - Specimens description

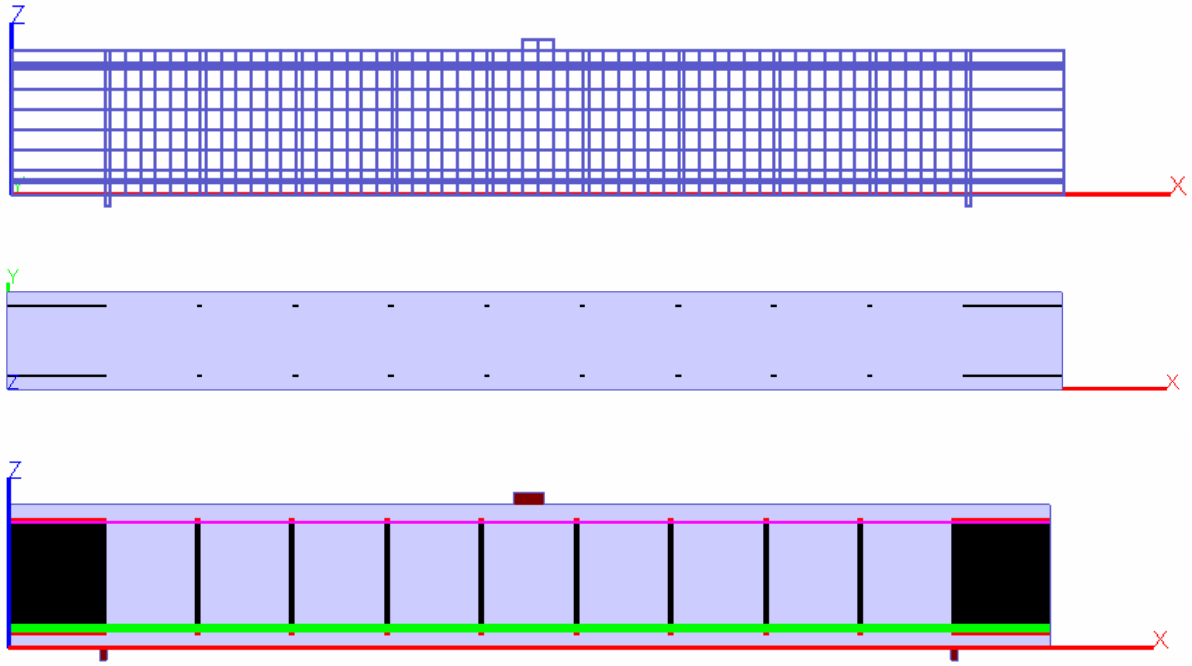
Series	Specimen	Web reinforcement	Web reinforcement arrangement	Concrete Grade (MPa)
A	RA1	2Ø6 c/c 200 mm	Closed loop	30
	RA2	1Ø6 c/c 100 mm	Closed loop	
	RA3	2Ø6 c/c 200 mm	Single leg Staggered	
	RA4	1.5 Ø 6 c/c 150 mm	Closed loop	
	RA5	3Ø6 c/c 300 mm	Closed loop	
B	RB1	2Ø6 c/c 200 mm	Closed loop	15
	RB2	1Ø6 c/c 100 mm	Closed loop	
	RB3	2Ø6 c/c 200 mm	Single leg Staggered	
	RB4	1.5 Ø6 c/c 150 mm	Closed loop	

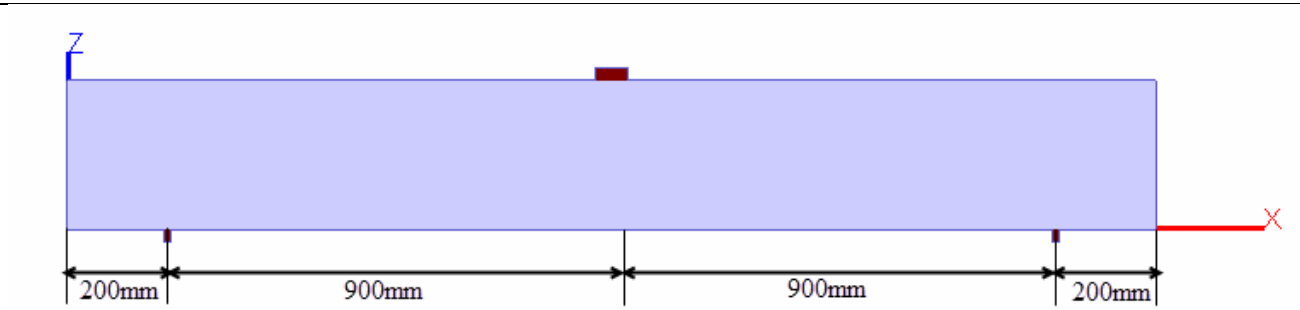
	RB5	3Ø6 c/c 300 mm	Closed loop	
C	RC1	2Ø6 c/c 200 mm	Closed loop	45
	RC2	1Ø6 c/c 100 mm	Closed loop	
	RC3	2Ø 6 c/c 200 mm	Single leg Staggered	
	RC4	1.5 Ø 6 c/c 150 mm	Closed loop	
	RC5	3Ø6 c/c 300 mm	Closed loop	


Z
X
200mm
900mm
900mm
200mm

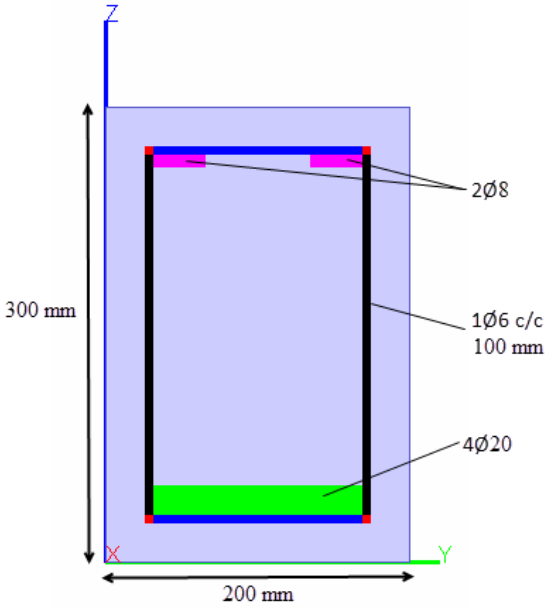
RA1, RB1, RC1

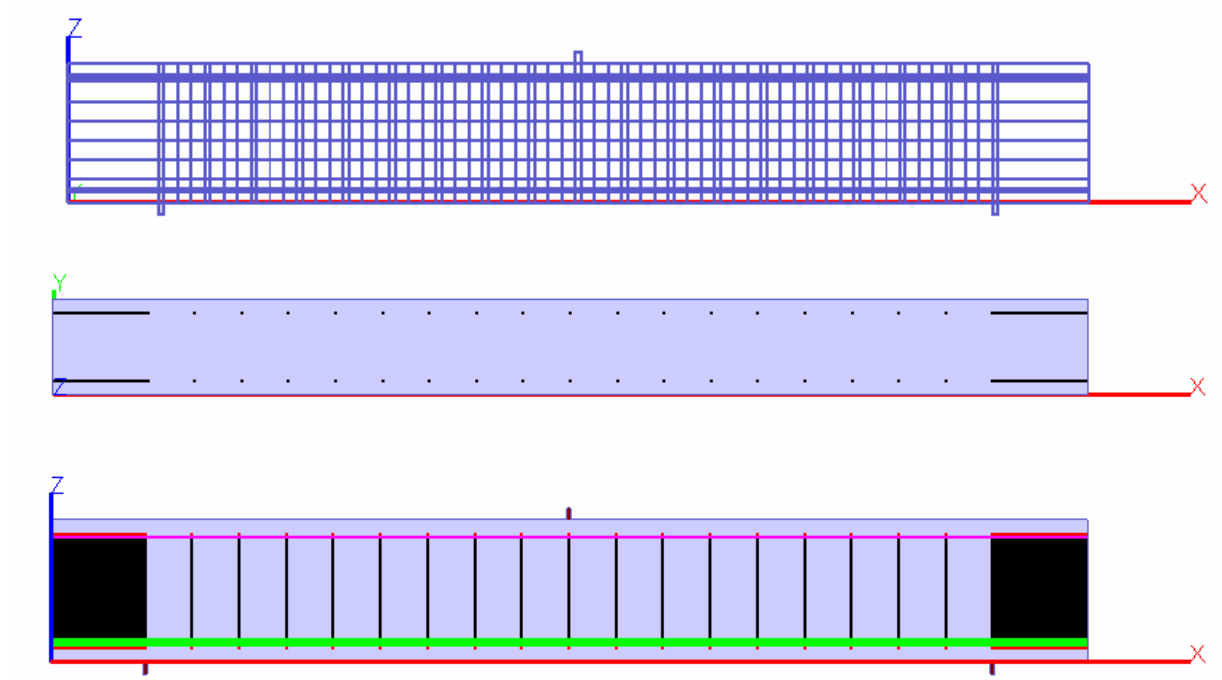

Z
2Ø8
300 mm
2Ø6 c/c
200 mm
4Ø20
X
Y
200 mm

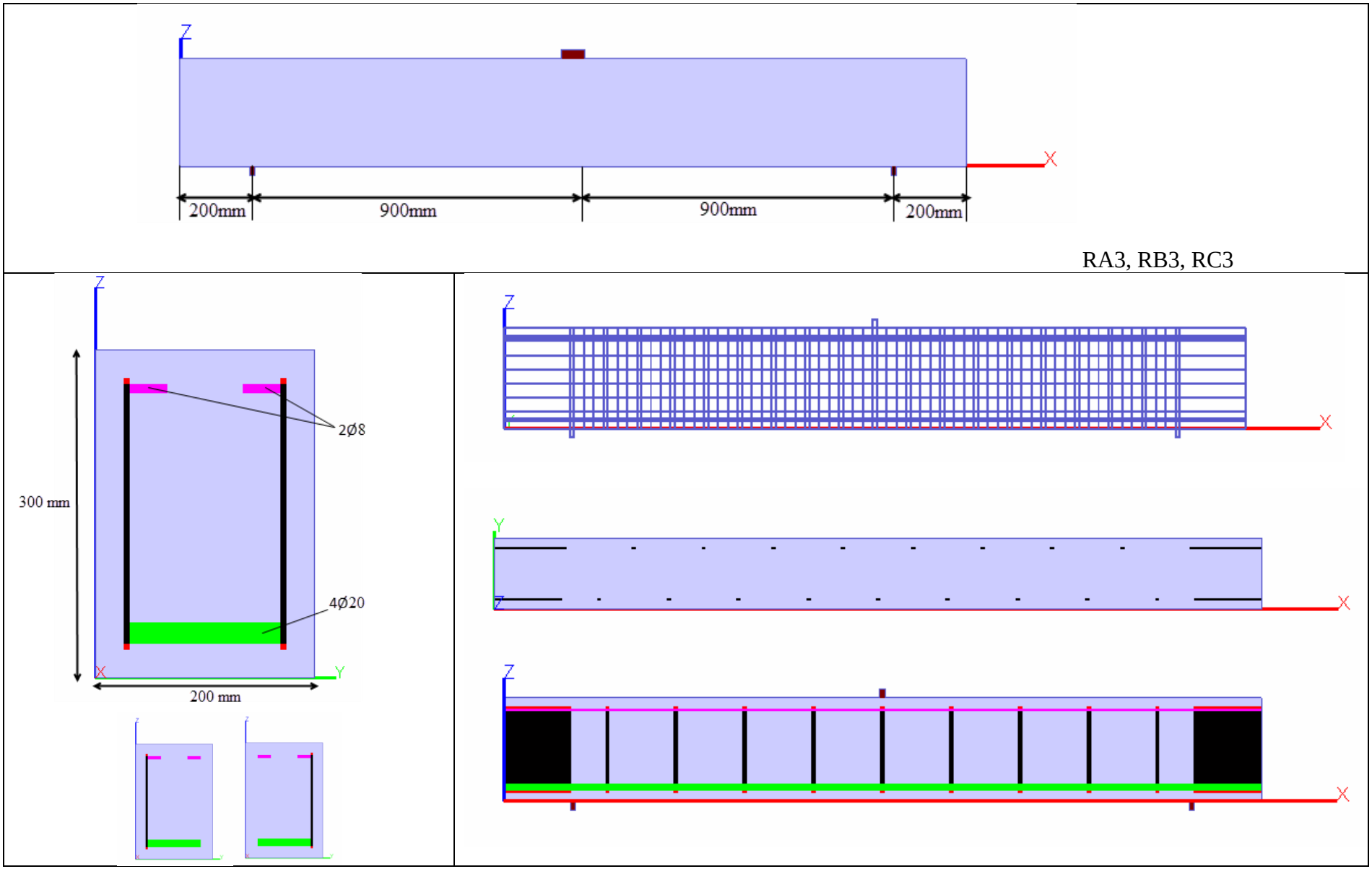

Z
X
Y
Z
X
Z
X

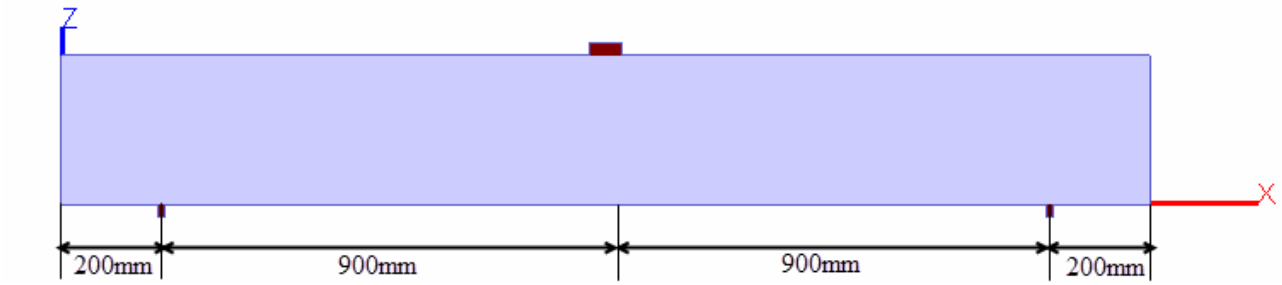

Z
X
200mm
900mm
900mm
200mm

RA2, RB2, RC2

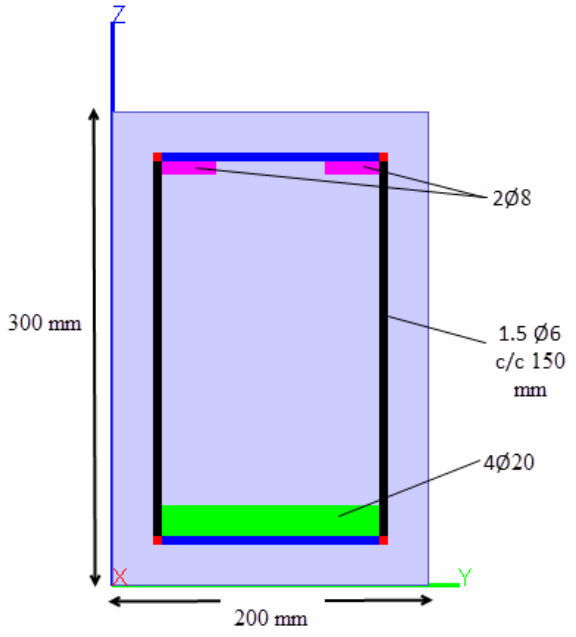

Z
2Ø8
300 mm
1Ø6 c/c
100 mm
4Ø20
X
Y
200 mm

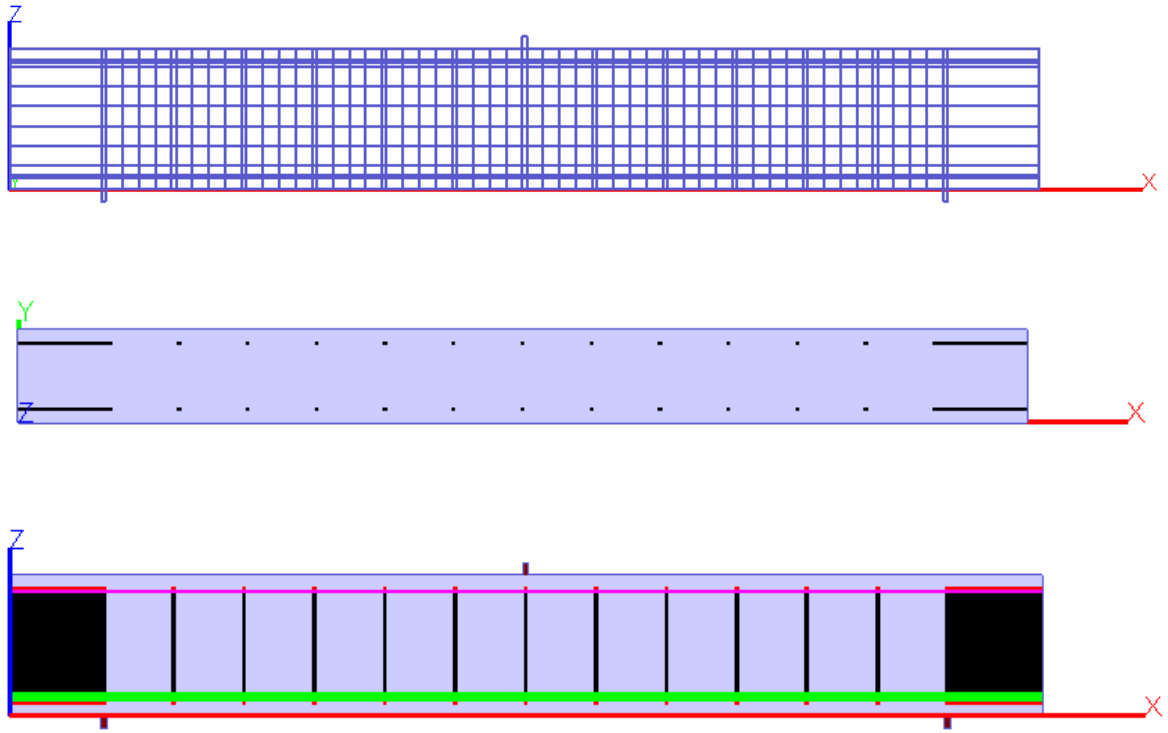

Z
X
Y
X
Z
X

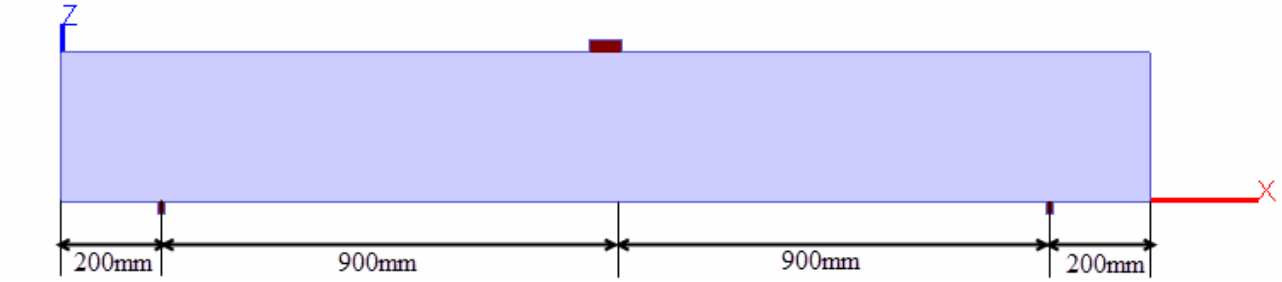

Z
X
200mm
900mm
900mm
200mm
RA3, RB3, RC3
Z
300 mm
2Ø8
4Ø20
X
Y
200 mm
Z
X
Y
Z
X
Z
X


Z
X
200mm
900mm
900mm
200mm

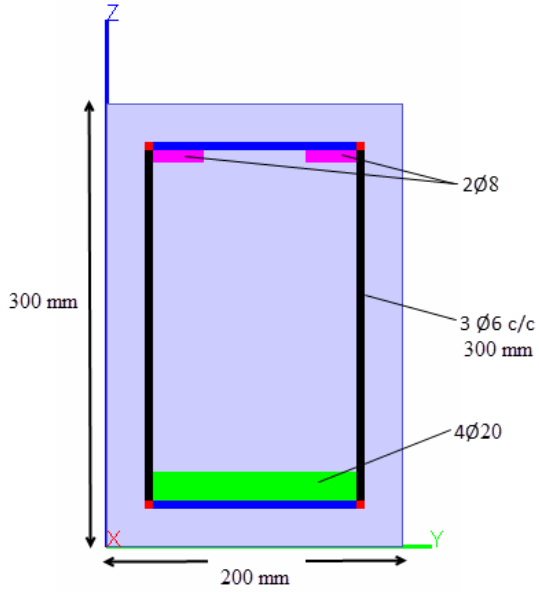
RA4, RB4, RC4

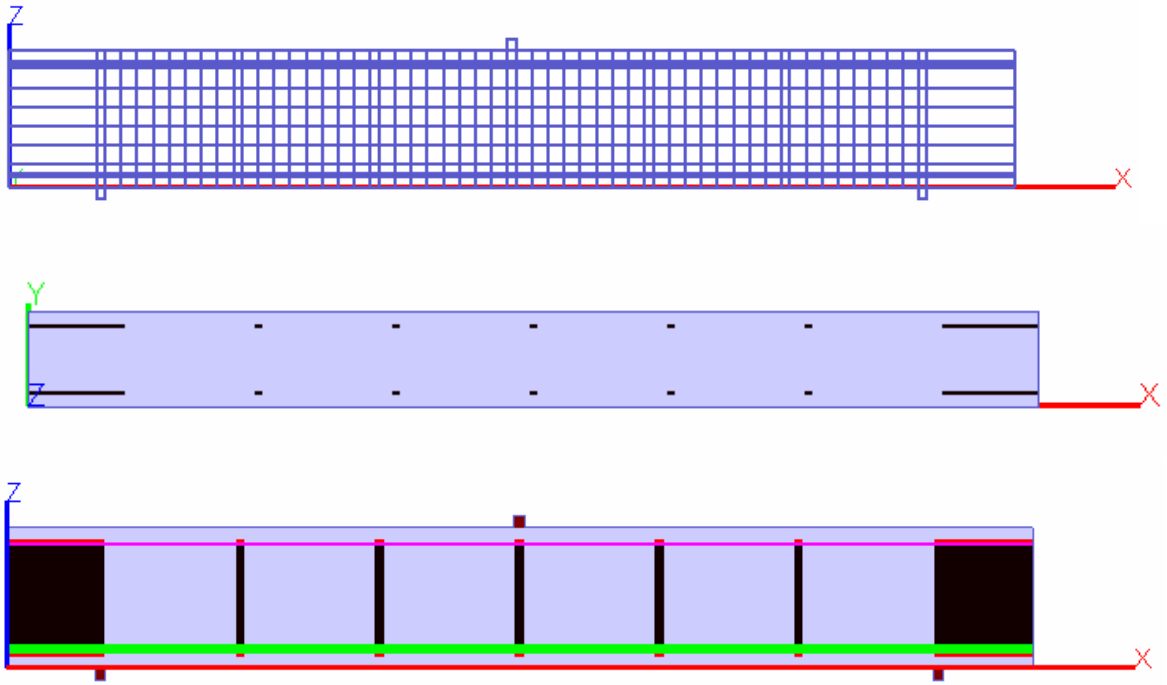

Z
2Ø8
300 mm
1.5 Ø6
c/c 150
mm
4Ø20
X
Y
200 mm


Z
X
Y
Z
X
Z
X


Z
X
200mm
900mm
900mm
200mm

RA5, RB5, RC5


Z
2Ø8
300 mm
3 Ø6 c/c
300 mm
4Ø20
X
Y
200 mm


Z
X
Y
Z
X
Z
X

5.3 Materials

Concrete grade of 30, 15 and 45 MPa was considered for series A, B, and C respectively. The tensile capacity and modulus of elasticity of the concrete was calculated by a formula recommended in [**12**]

$$f_t = 0.33\sqrt{f_c} \quad (44)$$

$$E_c = 3320\sqrt{f_c} + 6900 \quad (45)$$

Mechanical properties for concrete in all the three series of specimens in presented in Table 5-2.

Table 5-2 – Mechanical property of concrete

	Concrete Grade (MPa)		
	15	**30**	**45**
Initial Stiffness (kgf/cm^2)	201409.834	255702.231	297362.253
Compressive strength (kgf/cm^2)	152.905	305.810	458.715
Tensile strength (kgf/cm^2)	13.028	18.425	22.566
Poisson's ratio	0.2	0.2	0.2
Unit weight (kgf/cm^3)	0.0025	0.0025	0.0025

Two types of reinforcing steel bars were used in the specimens. A normal strength reinforcing bar was used for the shear reinforcements and top reinforcements and a high strength reinforcing bar was used for the longitudinal reinforcements. Detail property of the reinforcing steel bars is described in Table 5-3.

Table 5-3 – Mechanical property of reinforcement bar

	Longitudinal bar	**Top and web reinforcement**
Initial Stiffness (kgf/cm^2)	2000000	2000000
Yield strength (kgf/cm^2)	18119.07	2463.389
Tension rupture strength (kgf/cm^2)	19541.52	3157.35
Tension rupture strain	0.12	0.12
Poisson ratio	0.2	0.2
Unit weight (kgf/cm^3)	0.0078	0.0078

5.4 Modeling

The analysis was performed using the multi - directional fixed crack FE framework. All steel bars were modeled as embedded smeared reinforcement inside the elements. Concrete

elements without steel bars were modeled as plain concrete element. Concrete with steel reinforcement was modeled as RC elements characterized by tension stiffening. Loading plates and support bearings were modeled as elastic elements characterized by unyielding behavior.

5.5 Support condition and loading

The beams were simply supported with 1.8 m distance between the supports. Elastic bearings were used at the support and at the point of load application. To capture the post peak behavior of the beams, a displacement controlled analysis was performed by applying a downward displacement of 0.02 cm per minute for 80 load steps at the mid span.

CHAPTER 6 RESULT AND DISCUSSION

6.1 Result from experiment

6.1.1 Result

In all the three specimens, a typical shear failure was observed. First small flexural cracks formed at the bottom of the mid span but after a certain interval of time diagonal cracks become visible and finally the width of this diagonal cracks increased and the beams failed. All of the three beam specimens failed due to yielding and rupture of the web reinforcements.



Figure 6-1 – Initiation of diagonal cracks



Figure 6-2 – Diagonal tension failure in Specimen B-2

As was mentioned in section 4.4, Load was applied using a medium sized hydraulic jack. The hydraulic jack was set on the beam and it gets the reaction necessary to apply load from the rigid steel frame above it. However during experiment, when the beam deflects, the hydraulic jack moves downward with the beam and losses its reaction from the rigid frame. This result a decrease in the registered load at some points after the experiment was started. This phenomenon was a problem in specimens B1 and B2 and can easily be captured from the cyclic kind of pattern in the load deflection diagram of specimens B1 and B2.

Specimen B3 was not symmetrical in terms of the arrangement of web reinforcement longitudinally. Half of the beam contained vertical leg of stirrups aligned in a staggered mode. To study the effect of staggering the stirrups in relation to confinement, half of the beam contained closed stirrups aligned at 45 degree in the horizontal plane to have a staggered arrangement. During the experiment, it was observed that the portion of the beam which has only vertical staggered stirrups failed before a major diagonal crack was observed in the other half.

The load deflection diagram for the three specimens is shown in the following figures.

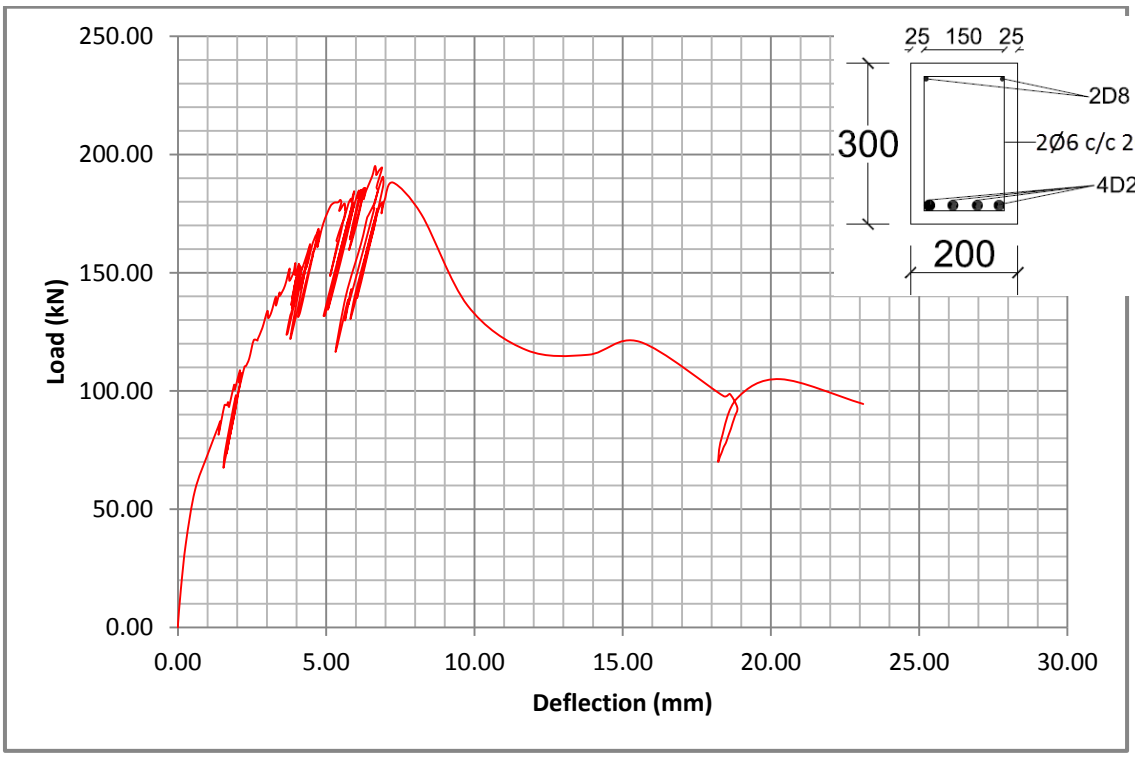


Figure 6-3 – Load – Deflection diagram for specimen B1

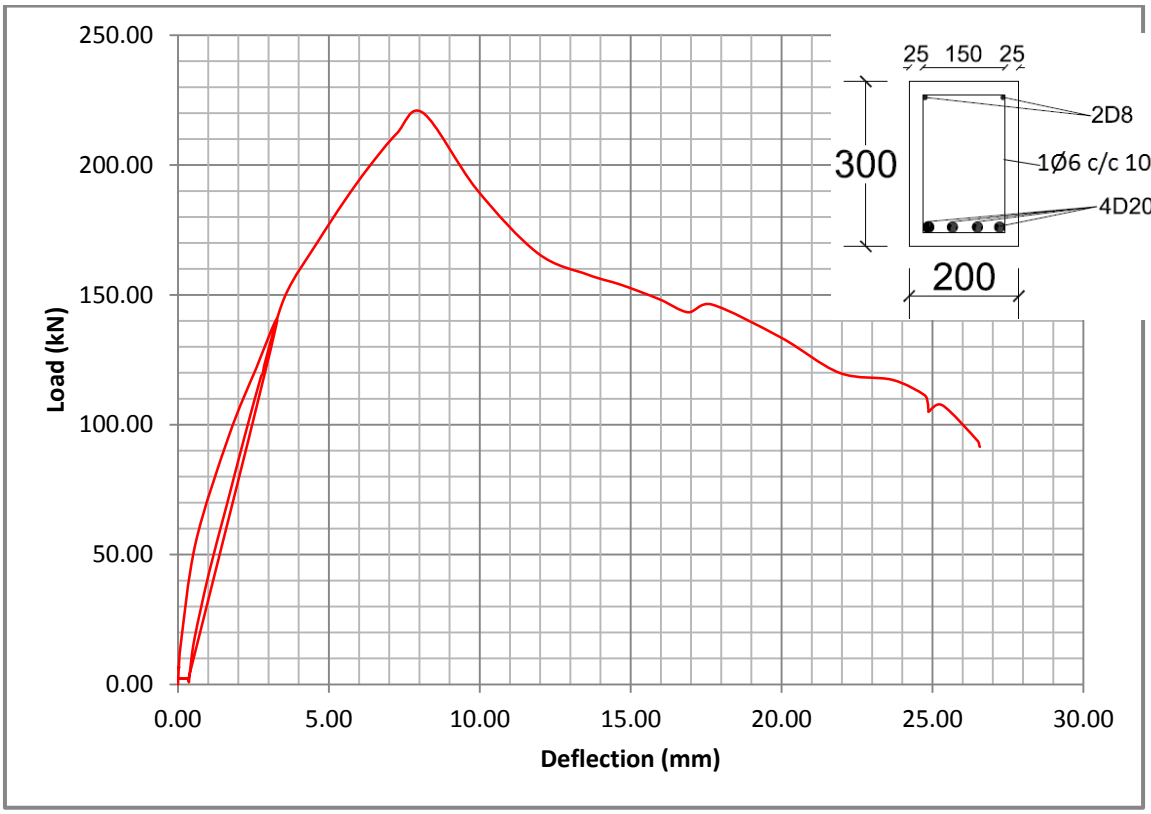


Figure 6-4 – Load – Deflection diagram for specimen B2

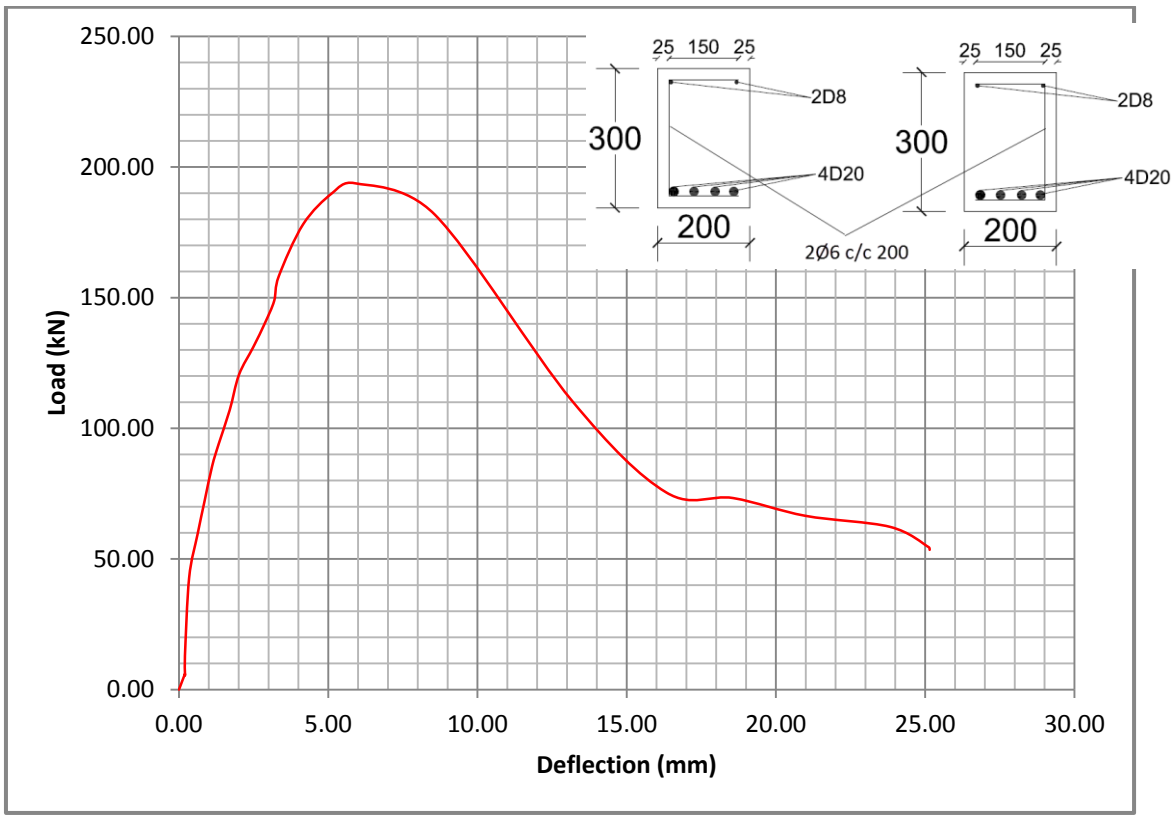


Figure 6-5 – Load – Deflection diagram for specimen B3

6.1.2 Effect of spacing of web reinforcement

As can be observed from the Load – Deflection diagrams, providing Ø6 c/c 100 mm resulted a capacity of 220 kN which is almost 30 kN higher than the capacity of 2Ø6 c/c 200 mm which was observed to have a capacity of about 190 kN. It is well known that slip of the stirrup through the concrete induces bond stresses which transfer force from the stirrup to the concrete between cracks. In order to form a crack within an effective concrete area around the stirrup, the force which has to be introduced to concrete by bond at the end of the transfer length should exceed the cracking strength of concrete. Providing smaller spaced stirrups decreases the crack spacing and crack width. The reason for this behavior is the decreasing effective concrete area, in which shear crack width is controlled by the stirrup, and hence the increasing bond effect between the stirrups and the surrounding concrete. Increasing the bond effect results in reducing the transfer length (or crack spacing) in which the forces to cause crack are transferred into the concrete between cracks by the bond stresses.



Figure 6-6 – Shear opening displacement (width) in spacemen B-1

6.1.3 Effect of arrangement of web reinforcement

The study of effect of arrangement of web reinforcement was initiated from the hypothesis that staggering the stirrups might orient the shear failure diagonal cracking plane to an inclined plane in comparison to the vertical plane of diagonal cracking in case of the normal arrangement of web reinforcement. This hypothesis was not proven to be true during the experiment.

The experimental result for the staggered arrangement (B3) has shown almost similar ultimate load capacity with specimen B2. However, half of this specimen (B3) which had vertical leg staggered stirrups failed before a major diagonal crack was observed on the other

half. This shows that, providing a confinement to a staggered arrangement might result a boost on the shear capacity. This increment in shear capacity can be justified from the reason outlined in section 6.1.2.

Examining the two unsymmetrical halves, it can be concluded that providing some confinement to a staggered arrangement results an increase in shear capacity. The reason for this statement is as follows. Shear crack width in RC members are usually accompanied by slip along shear cracks which create shear transfer by aggregate interlock. Slip which is related to shear opening displacement (width) is a main factor for fracturing of shear reinforcement. In further studies (Hassan and Ueda 1987; Hassan *et al*. 1991), it was reported that shear crack opening displacements are not only produced by elongation of vertical leg stirrup, but also are affected by slip of stirrup hooks and elongation of horizontal leg of stirrup which causes slip at the stirrup bent portion. Thus providing a closed stirrup in a staggered configuration reduces the slip and thus decreases the fracturing of aggregates by allowing mobilization of aggregate interlock with a small amount of slip.



Figure 6-7 – Slip along shear cracks in specimen B-2

6.2 Result from finite element analysis using DuCOM-COM3

6.2.1 Result

The load deflection diagram for the described specimens in section 5.2 is presented below. The load deflection diagrams are plotted for the three series separately to compare the effect of spacing and configuration of stirrups for different concrete grades. Series A, B, and C, are of concrete grade 30MPa, 15MPa and 45MPa respectively.

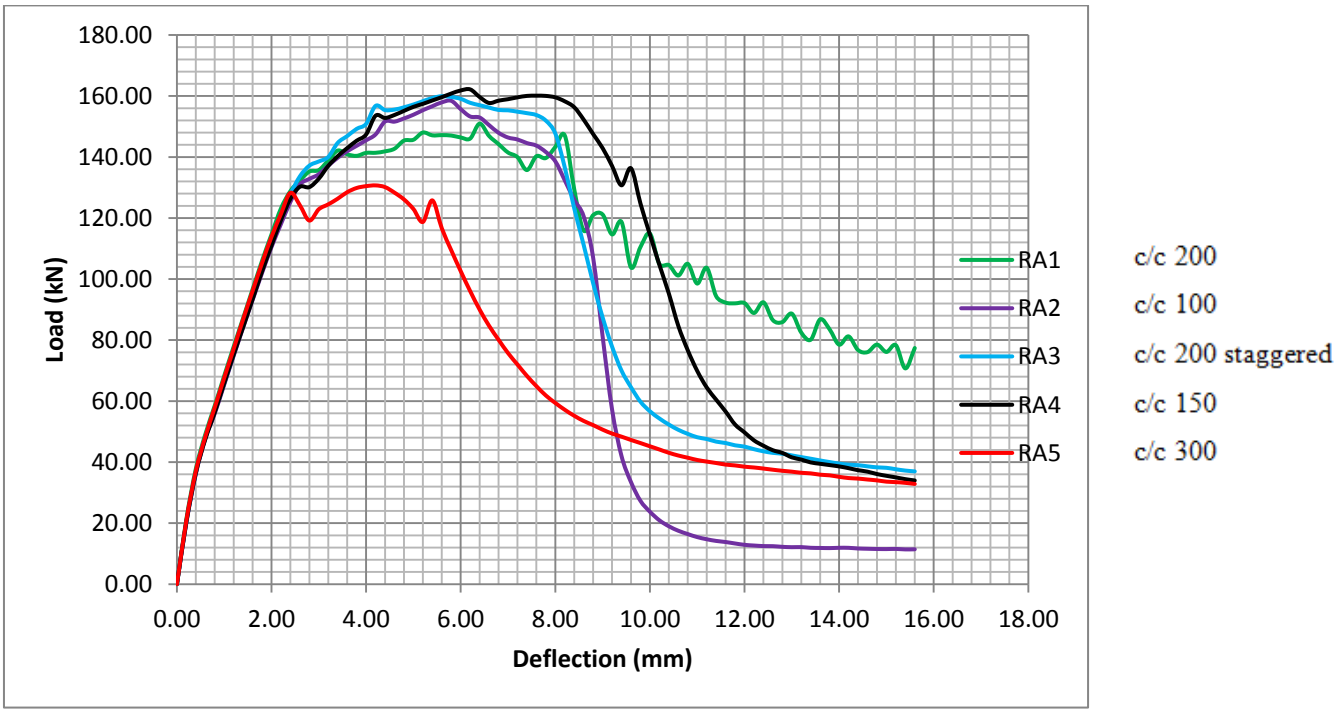


Figure 6-8 – Load-Deflection diagram for series-A beams

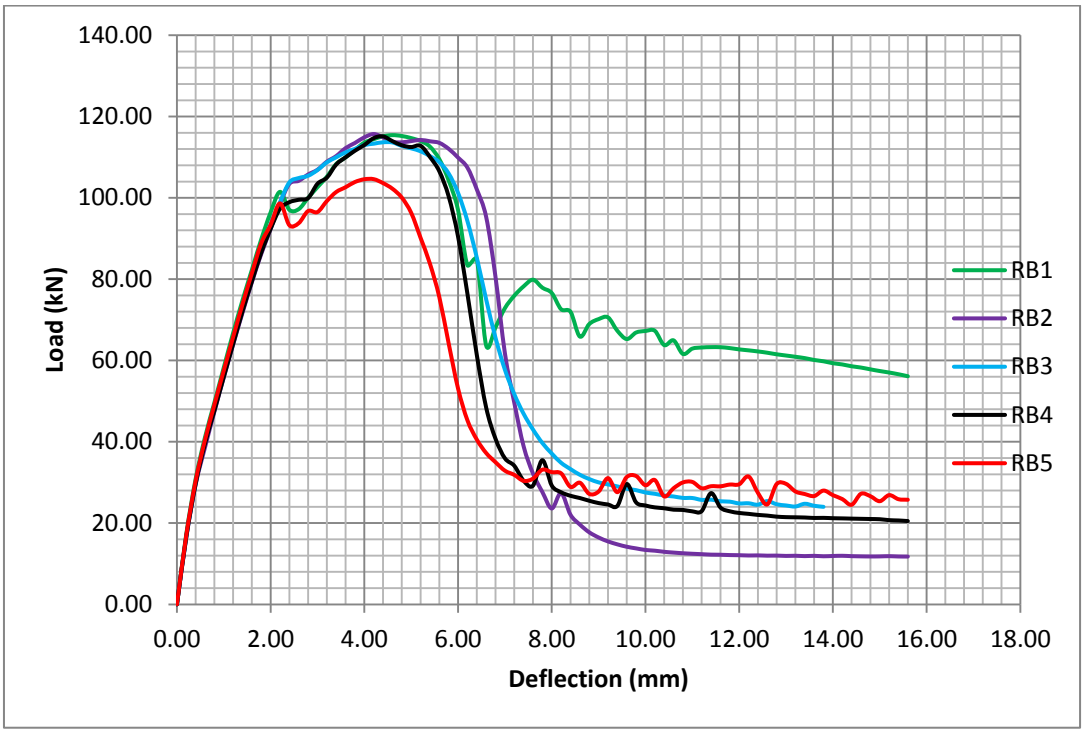


Figure 6-9 – Load-Deflection diagram for series-B beams

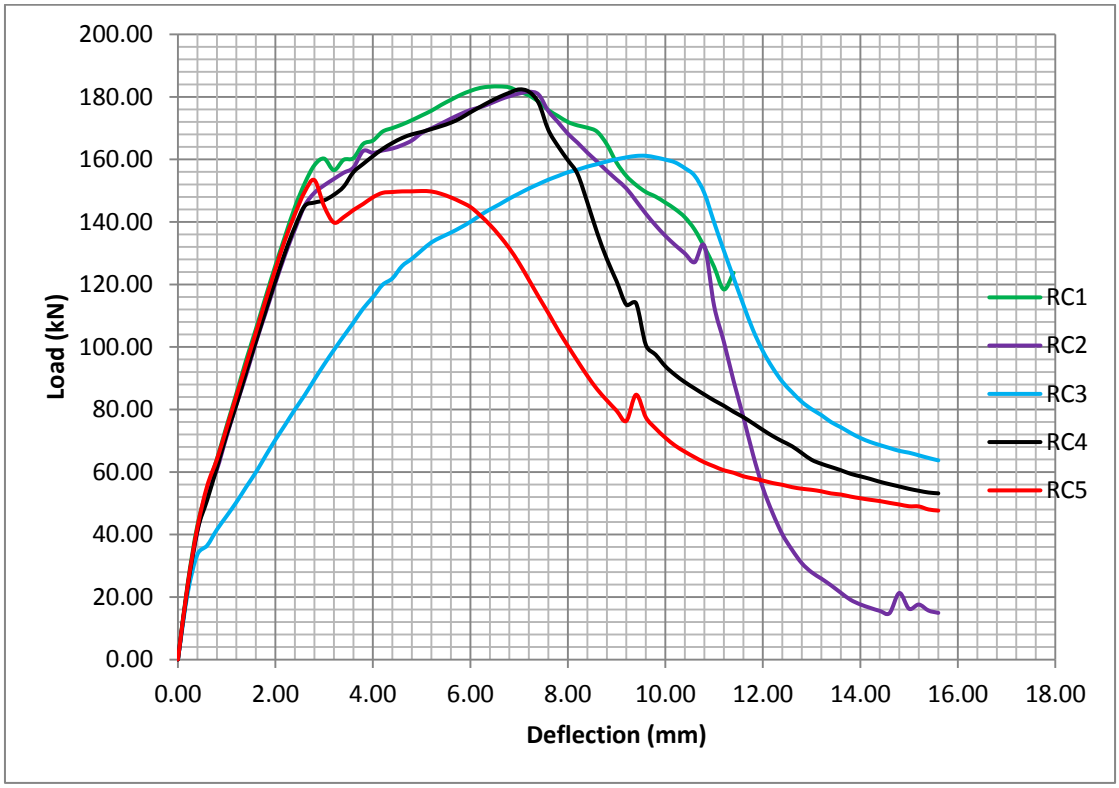


Figure 6-10 – Load-Deflection diagram for series-C beams

6.2.2 Effect of spacing and arrangement of stirrups

The effect of spacing can be studied by comparing the ultimate capacity of specimens whose spacing varied from 150 to 300 mm. For the cross section of the beam specimens, EN 2 -1-1, 2004 provision sets a maximum spacing of 200 mm. As can be seen from the load deflection diagram the beams whose spacing is below the maximum spacing set by the code failed at almost the same capacity except for Series-A which has about 10 kN difference. This shows that the finite element modeling did not capture the effect of spacing as was assumed. This may be because the effect of tension stiffening in the concrete surrounding the web reinforcement was not clearly modeled. While modeling the specimens, only the narrow cubic part of the mesh that contained the web reinforcement was assigned a tension stiffening factor for a stiffened concrete. Other parts of the mesh were modeled as a plain concrete. However, in reality, some part of the area of surrounding concrete will be stiffened by the web reinforcement and providing a densely spaced reinforcement means allowing most part of the concrete to be stiffened by the web reinforcement and this results closely spaced cracks with small crack width. From the basic theory of shear transfer, as the crack width decreases, the transferred shear through aggregate interlock increases which in turn outcomes increase in shear capacity.

From the series, Series-B exhibited a load deflection diagram which is almost similar for all the different arrangement of stirrups. This might be because series-B has the minimum concrete grade (C-15) and from the theory of shear transfer, as the concrete grade decreases the ultimate shear capacity will tend to be governed by crushing of inclined struts and as failure is not initiated by yielding of stirrups the arrangement of web reinforcement in these kinds of specimens might not play a great role.

For the beam specimen that contained stirrups spaced above the maximum spacing, it can be seen that there was a difference in ultimate capacity of 30kN in Series-A (C30) and Series-C (C45).

6.3 Comparison between result from analytical simulation and experiment

The analytical simulation on DuCOM-COM3 involved 15 beam specimens under three series of concrete grades. Out of the 5 specimens in each series, three of them were identical to the specimens that were tested during the experimental program. This was done intentionally to

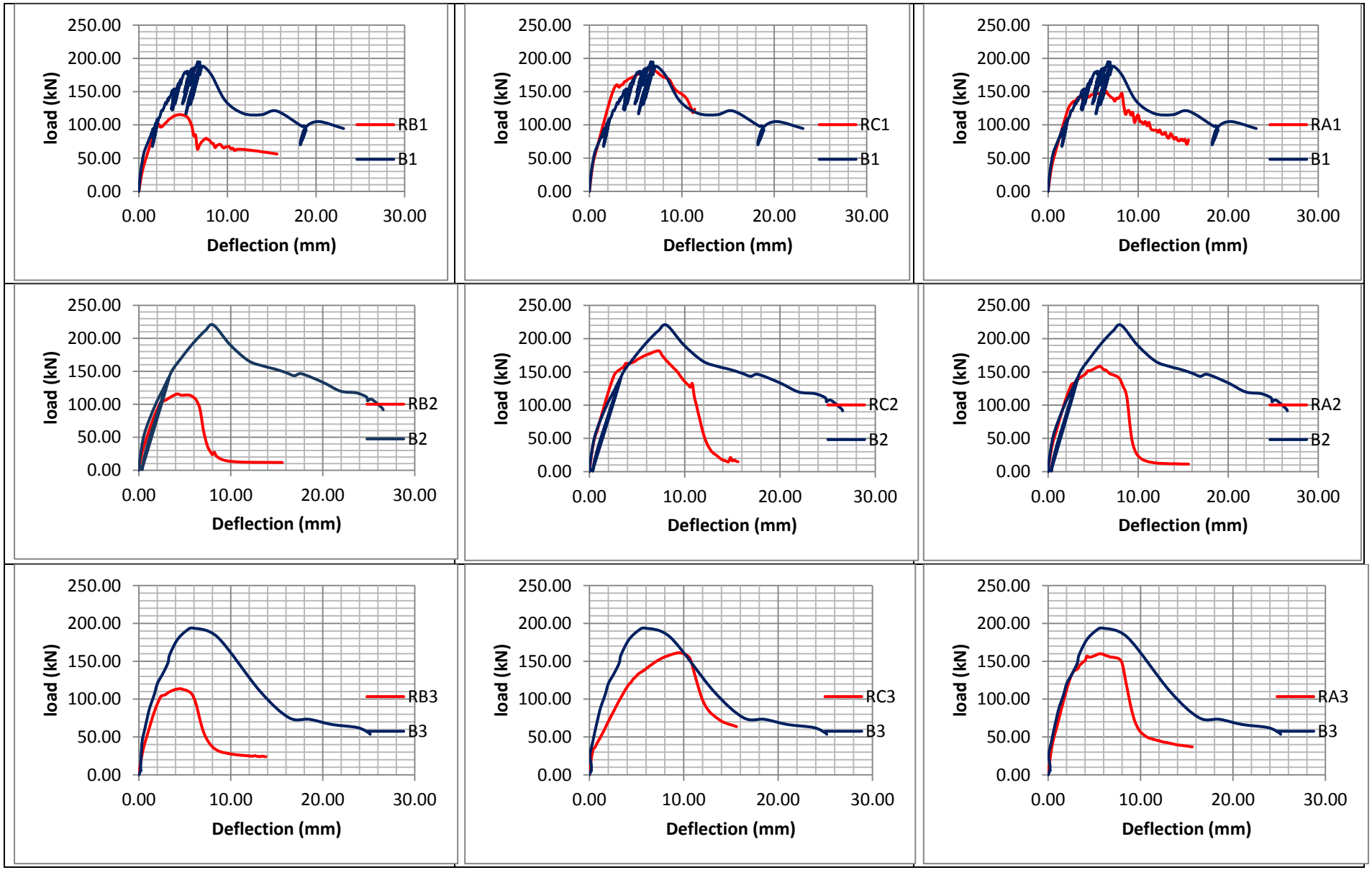
verify the analytical simulation by the experimental result. However, two major problems occurred in this plan.

One of the problems is that the concrete grade that was registered from the experiment by testing cylinder specimens was not found to be acceptable because the concrete grade in the 9 cylinder samples varied erratically. On the other hand the mix design was done for C-30 concrete after having a trial mix which has achieved over 38 MPa but the average compressive strength from the cylinder samples was only 14.33 MPa.

The other problem is that the analytic simulation was not able to capture the effect of spacing and arrangement of web reinforcement due to the fact that the tension softening and tension stiffening zone could not be managed to be introduced in the plane and reinforced concrete zones.

Thus, to avoid the first problem, the result from the experiment is compared with the analytical simulation results for the three classes of concrete in the three series. Comparison between load- deflection diagram for these three series of specimens and experimental results is shown in the figures below.

Note: Series A, B and C are of concrete grade 30, 15 and 45 MPa respectively.


250.00
200.00
150.00
100.00
50.00
0.00
load (kN)
0.00
10.00
20.00
30.00
Deflection (mm)
RB1
B1
RC1
B1
RA1
B1
RB2
B2
RC2
B2
RA2
B2
RB3
B3
RC3
B3
RA3
B3

From the above figures it can be observed that both the experiment and the analytical simulation exhibited a typical shear failure. However the ultimate capacity from the load-deflection diagram did not match for any of the series with the experimental result although there is some correlation in the initial curve for Series-C. This could be because the tensile strength of concrete that was used for the analytical simulation was the lower bound tensile strength given in literatures and shear capacity of beams are highly influenced by the tensile capacity of the concrete. But further investigation is recommended to study the difference between these two results.

CHAPTER 7 CONCLUSION AND RECOMMENDATION

7.1 Conclusion

In this research effect of spacing and arrangement of stirrups has been studied by reviewing well-known Building Codes and their basic models, through experimental program on three shear-critical specimens, and through analytical simulation of 15 shear-critical beam specimens. After examining these analyses, the following points are put forward.

1. Building code provisions of shear capacity calculation doesn't consider spacing and arrangement of stirrups as a factor affecting the shear capacity of beams. This resulted from the simplifications made to the basic shear capacity calculation models (truss analogy and MCFT) to make these theories easily adoptable for design purpose.
2. The experimental program revealed that shear behavior of beams is affected by the spacing and arrangement of web reinforcement especially for beams whose failure is initiated by yielding and rupture of stirrups.
3. Beams with web reinforcement spacing exceeding the limit of maximum (in accordance to Eurocodes' provision) spacing exhibited a drastic decrease in shear capacity.
4. Staggered configuration of web reinforcement gives comparably higher shear capacity if sufficient confinement is provided, as compared to the normal configuration of stirrups

7.2 Recommendation

1. Whenever possible, providing smaller spacing of web reinforcement while designing should be encouraged.
2. The effect of spacing of stirrups on beams of larger size should be further investigated because the maximum spacing provision in building codes is usually directly proportional to the effective depth which in turn gives the designer a lot of option for spacing of stirrups in larger size beams.
3. Since shear behavior of beams is affected by different factors (longitudinal reinforcement ratio, shear span to depth ratio, size of the beam, concrete grade …..),

this study should be further expanded to see the effect of spacing and arrangement of stirrups in relation to these factors.

4. Providing closed stirrup aligned to make 45^0 on its horizontal leg to get a staggered arrangement should be studied as another option of stirrup configuration to enhance shear capacity and crack control.

REFERENCES

[1] M. Peter, "Truss Models in Detailing," 1985.

[2] C. E. Bentz, F. J. Vecchio, and M. P. Collins, "Simplified Modified Compression Field Theory for Calculating Shear Strength of Reinforced Concrete Elements," vol. ACI Structural Journal, no. July-August, 2006.

[3] M. Aruna, "Shear Behavior of Concrete Beams Reinforced with High Performance Steel Shear Reinforcement," 2008.

[4] M. Zakaria, T. Ueda, Z. Wu, and L. Meng, "Experimental Investigation on Shear Cracking Behavior in Reinforced Concrete Beams with Shear Reinforcement," 2009.

[5] ASCE-ACI Committee 445, "Recent Approaches to Shear Design of Structural Concrete," *American Society of Civil Engineers*, December 1998.

[6] A. H. Nilson, D. Darwin, and W. C. Dolan, *Design of Concrete Structures*, 14th ed. New York, US: Mc Graw Hill Companies, 2010.

[7] K. J. Weight and J. G. Macgregor, *Reinforced Concrete Mechanics & Design*, 6th ed. New Jersey, US: Pearson Education, 2012.

[8] M. Ghoneim and M. EL-Mihilmy, *Design of Reinforced Concrete Structures*, 2nd ed. Egypt: Cairo University, 2008.

[9] Transportation Reasearch Board Executive Commitee , "Simplified Shear Design of Structural Concrete Members," *NCHRP*, vol. NCHRP REPORT 549, 2005.

[10] AASHTO, *AASHTO LRFD BRIDGE DESIGN SPECIFICATIONS*. Washington, DC, US, 2012.

[11] M. P. Collins, E. C. Bentz, E. G. Sherwood, and L. Xie, "AN ADEQUATE THEORY FOR THE SHEAR STRENGTH OF REINFORCED CONCRETE STRUCTURES,"

2007.

[12] J. Vecchio Frank, "Analysis of shear-critical reinforced concrete beams," *ACI Structural Journal*, vol. 97, January - February 2000.

[13] ACI Commitee 318, "Building Code Requirements for Structural Concrete (ACI 318-14) AND Commentary on Building Code Requirements for Structural Concrete (ACI 318R-14)," American Concrete Institure, 2014.

[14] European Standard, "Eurocode 2: Design of Concrete Structures," European Commitee for Standardization, 1992.